

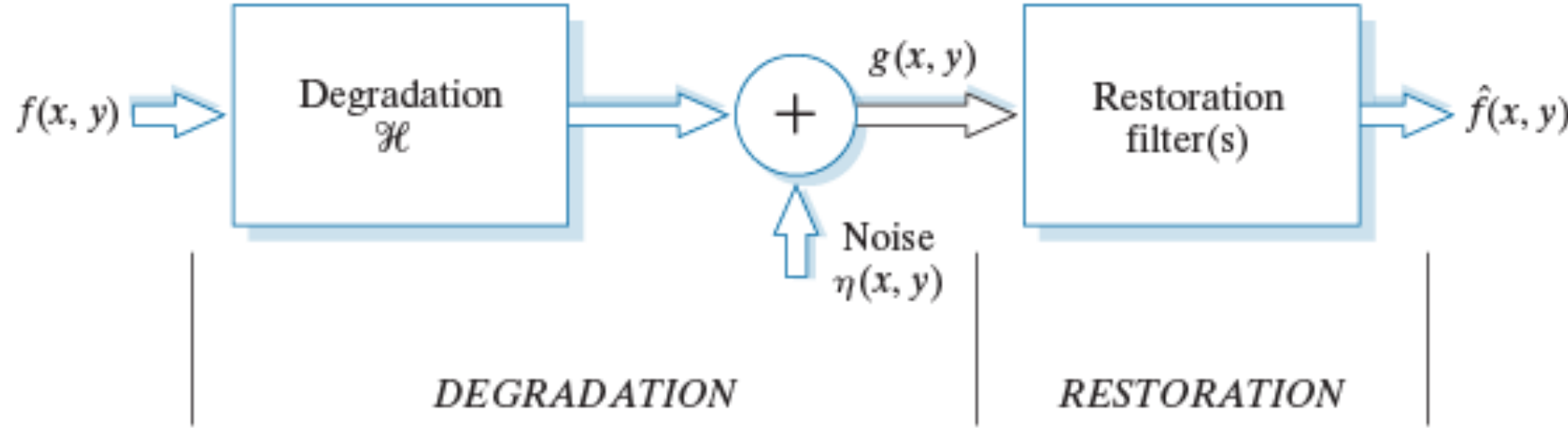
EE 5098 – Digital Image Processing

5. Image Restoration and Reconstruction

Image Restoration

- Image restoration: recover a degraded image by using a prior knowledge of the degradation
 - Model the degradation and applying the inverse process to recover the original image.
 - An objective process. (In contrast, image enhancement described in Chapters 3 and 4 is a subjective process.)
- Outlines
 1. Degradation model for digital image
 2. Restoration for a noise-only degradation process
 3. Interactive restoration method
 4. Inverse filtering approach
 5. Wiener Filter (LSE, MMSE filter)

Modeling of Image Degradation/Restoration Process



\mathbf{H} : Degradation function

η : Additive noise

If H is linear and position-invariant,

$$g(x, y) = h(x, y) \star f(x, y) + \eta(x, y)$$

In the frequency domain,

$$G(u, v) = H(u, v)F(u, v) + N(u, v)$$

Noise Sources

- ❑ The principal sources of noise in digital images arise during **image acquisition and/or transmission**
 - ✓ Image acquisition
 - For example, light levels, sensor temperature, etc.
 - ✓ Transmission
 - For example, lightning or other atmospheric disturbance in wireless network

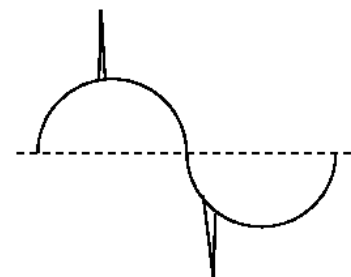
Spatial and Frequency Properties of Noise

- Spatial properties
 - Refer to parameters that define the spatial characteristics of noise
 - Whether the noise is correlated with image
- Frequency properties
 - Refer to the frequency content of noise
 - White noise: Fourier spectrum is constant
- With the exception of spatially periodic noise, we assume
 - Noise is independent of spatial coordinates
 - Noise is uncorrelated with the image

Noise Models

- **Gaussian (normal) noise**
 - Arises in an image due to factors such as electronic circuit noise and sensor noise due to poor illumination and/or high temperature.
 - Mathematically tractable
- **Rayleigh noise:** helpful in characterizing noise phenomena in range imaging
- **Erlang (gamma) noise:** find applications in laser imaging.
- **Exponential noise:** find applications in laser imaging.
- **Uniform noise:** may be the least descriptive of practical situations but it is quite useful as the basis for numerous random number generators.
- **Impulse noise:** found in situations where quick transients, such as faulty switching, take place during imaging.

We are concerned with the statistical behavior of the gray-level values of the noise component of the model. These values may be considered random variables characterized by a probability density function (PDF).



Impulse Noise

Gaussian Noise

The PDF of Gaussian random variable, z, is given by

$$p(z) = \frac{1}{\sqrt{2\pi}\sigma} e^{-(z-\bar{z})^2/2\sigma^2} \quad -\infty < z < \infty$$

where, z represents intensity

\bar{z} is the mean (average) value of z

σ is the standard deviation

70% of its values in the range $[(\mu - \sigma), (\mu + \sigma)]$

95% of its values in the range $[(\mu - 2\sigma), (\mu + 2\sigma)]$

Rayleigh Noise

The PDF of Rayleigh noise is given by

$$p(z) = \begin{cases} \frac{2}{b}(z-a)e^{-(z-a)^2/b} & \text{for } z \geq a \\ 0 & \text{for } z < a \end{cases}$$

The mean and variance of this density are given by

$$\bar{z} = a + \sqrt{\pi b / 4}$$

$$\sigma^2 = \frac{b(4 - \pi)}{4}$$

Erlang (Gamma) Noise

The PDF of Erlang noise is given by

$$p(z) = \begin{cases} \frac{a^b z^{b-1}}{(b-1)!} e^{-az} & \text{for } z \geq 0 \\ 0 & \text{for } z < 0 \end{cases}$$

The mean and variance of this density are given by

$$\bar{z} = b / a$$

$$\sigma^2 = b / a^2$$

Exponential Noise

The PDF of exponential noise is given by

$$p(z) = \begin{cases} ae^{-az} & \text{for } z \geq 0 \\ 0 & \text{for } z < a \end{cases}$$

The mean and variance of this density are given by

$$\bar{z} = 1/a$$

$$\sigma^2 = 1/a^2$$

A special case of the Erlang PDF with $b=1$.

Uniform Noise

The PDF of uniform noise is given by

$$p(z) = \begin{cases} \frac{1}{b-a} & \text{for } a \leq z \leq b \\ 0 & \text{otherwise} \end{cases}$$

The mean and variance of this density are given by

$$\bar{z} = (a + b)/2$$

$$\sigma^2 = (b - a)^2 / 12$$

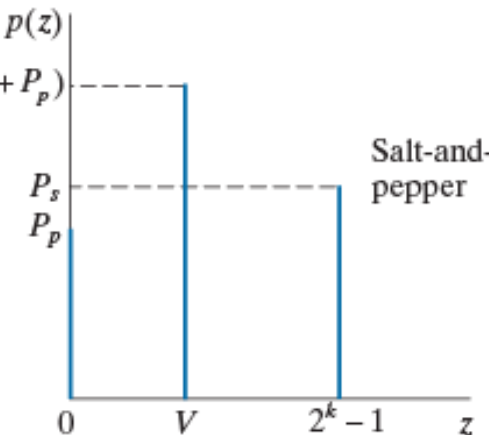
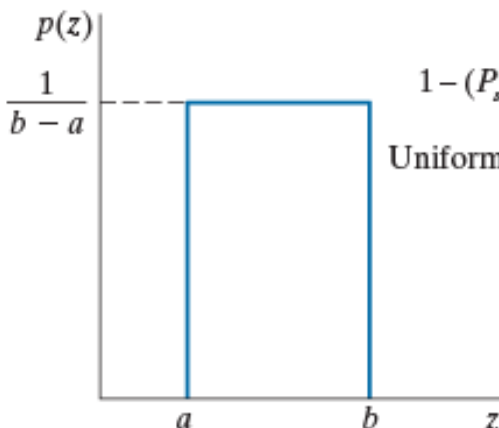
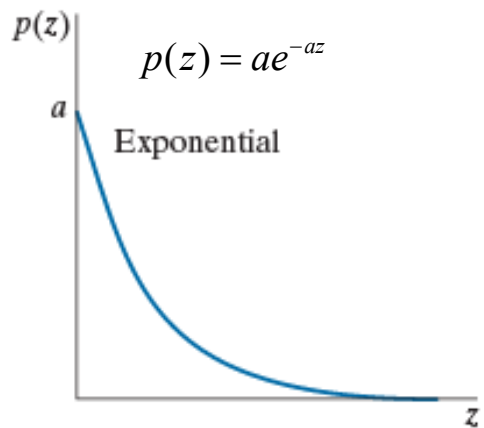
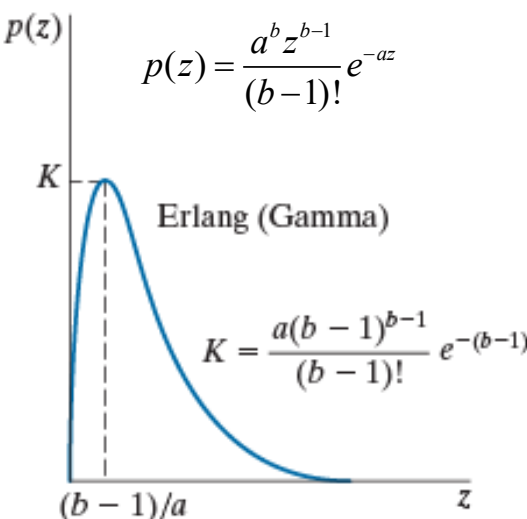
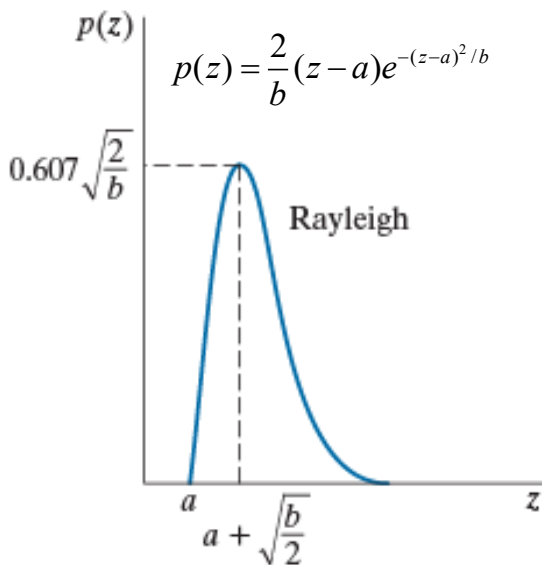
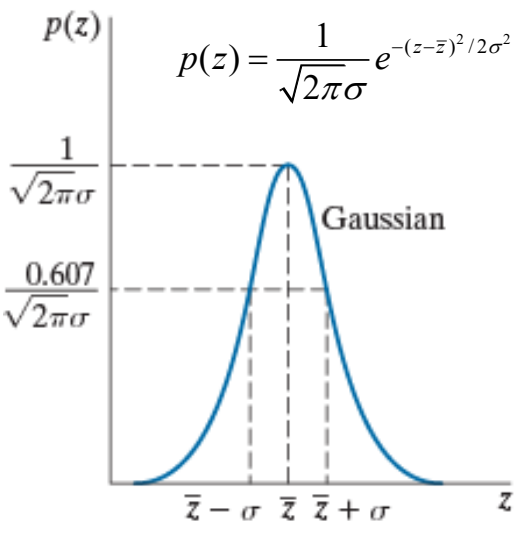
Salt-and-Pepper Noise

The PDF of this (bipolar) impulse noise is given by

$$p(z) = \begin{cases} P_s \text{ salt} & \text{for } z = 2^k - 1 \\ P_p \text{ pepper} & \text{for } z = 0 \\ 1 - P_s - P_p & \text{otherwise} \end{cases}$$

If either P_s or P_p is zero, the impulse noise is called *unipolar*.

Noise Models



a b c
d e f

FIGURE 5.2 Some important probability density functions.

Noisy Images and Their Histograms

Test Pattern

FIGURE 5.3

Test pattern used to illustrate the characteristics of the PDFs from Fig. 5.2.



Noisy Images and Their Histograms

Corrupted
with noise

原本沒 noise 應
該只有 3 個 bar (100%)
但 noise 太長這樣

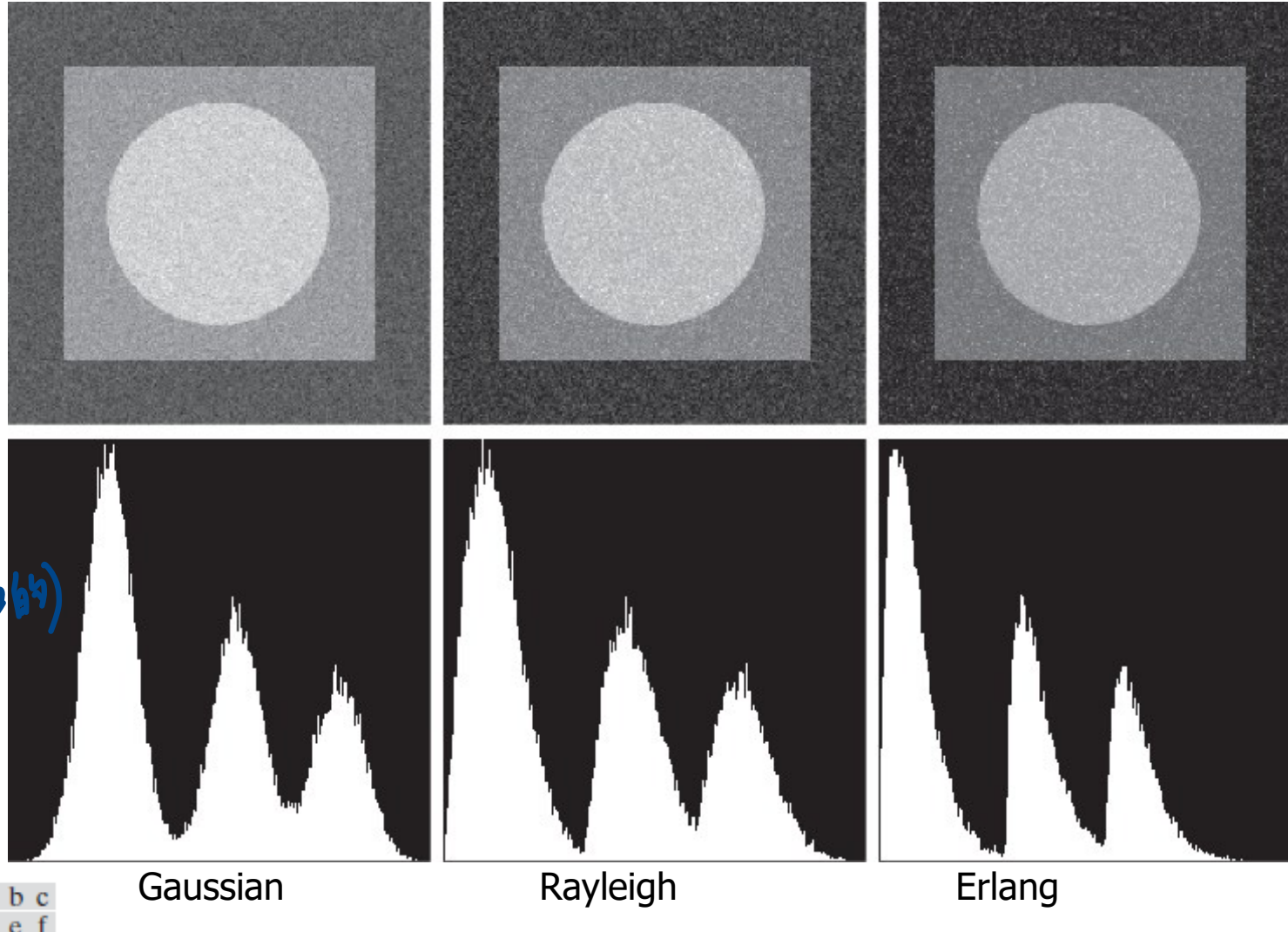


FIGURE 5.4 Images and histograms resulting from adding Gaussian, Rayleigh, and Erlang noise to the image in Fig. 5.3.

Noisy Images and Their Histograms

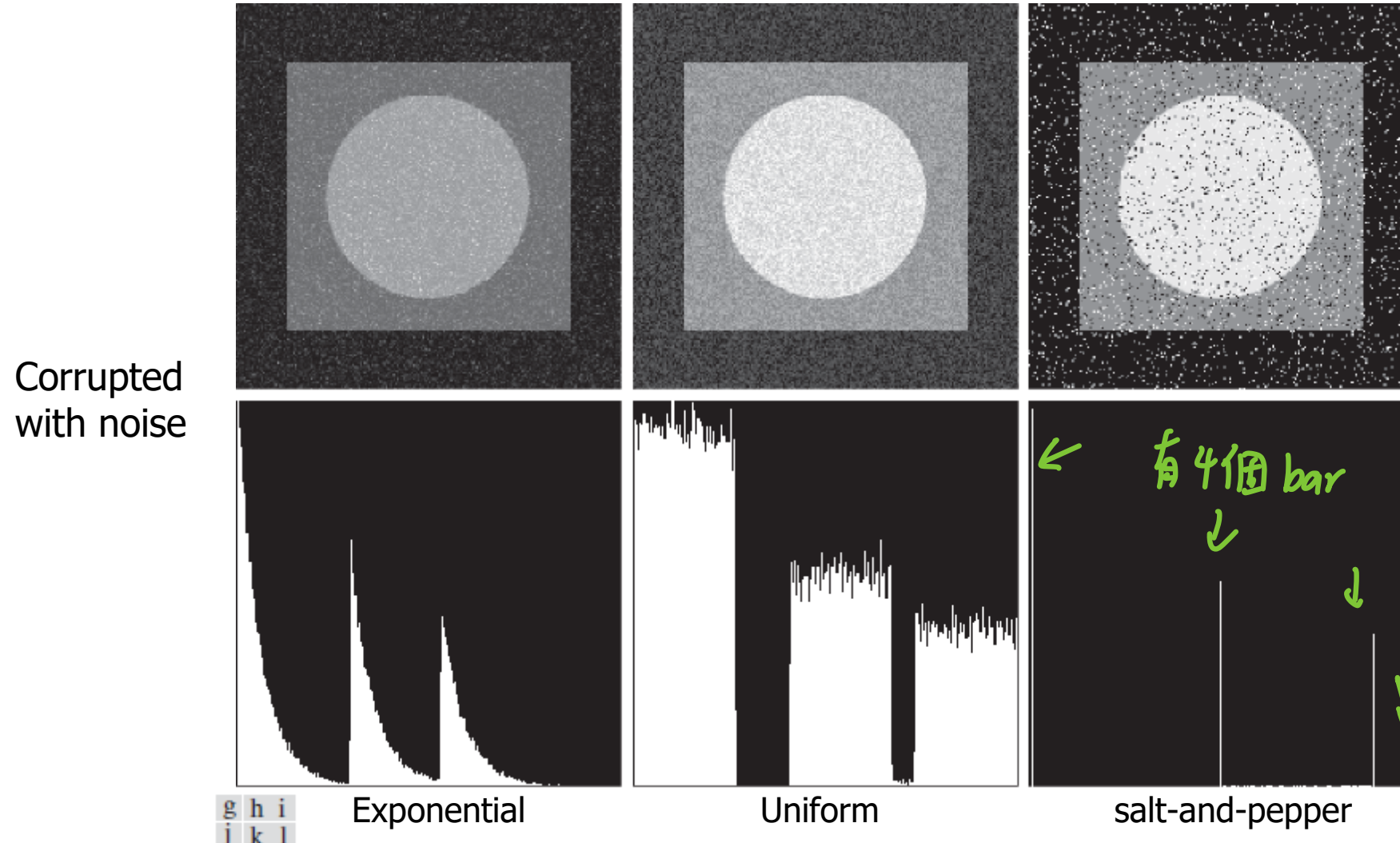


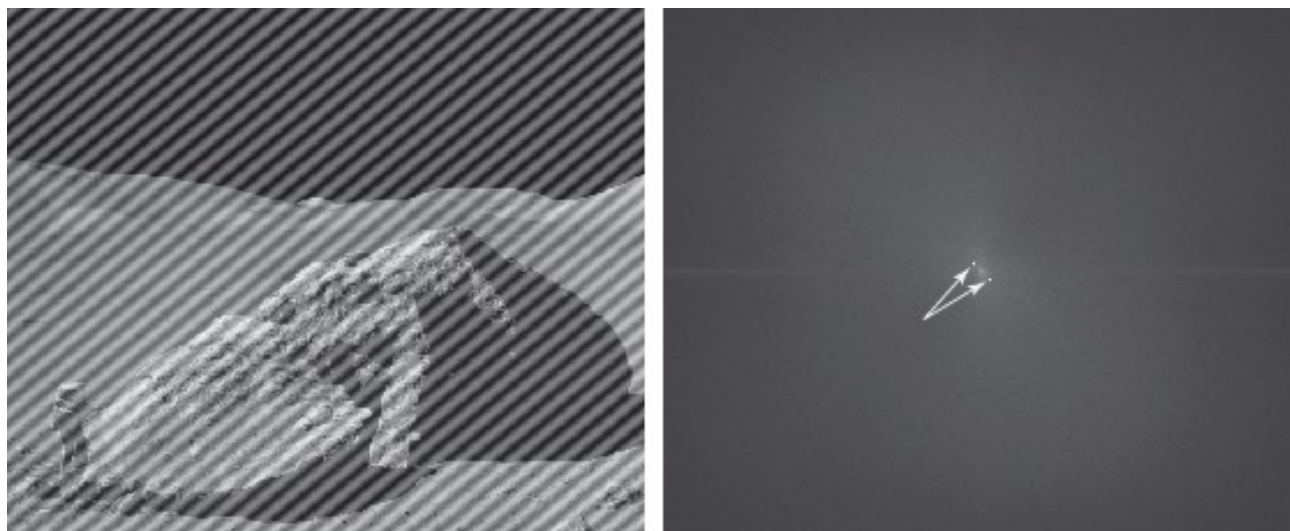
FIGURE 5.4 (continued) Images and histograms resulting from adding exponential, uniform, and salt-and-pepper noise to the image in Fig. 5.3. In the salt-and-pepper histogram, the peaks in the origin (zero intensity) and at the far end of the scale are shown displaced slightly so that they do not blend with the page background.

Periodic Noise

- ▶ Periodic noise in an image arises typically from **electrical or electromechanical interference** during image acquisition.
- ▶ The only type of **spatially dependent** noise considered here
- ▶ Periodic noise can be reduced significantly via **frequency domain filtering**

a b

FIGURE 5.5
(a) Image corrupted by additive sinusoidal noise.
(b) Spectrum showing two conjugate impulses caused by the sine wave.
(Original image courtesy of NASA.)



Two conjugate impulses

Estimation of Noise Parameters (1)

- Periodic noise → inspect its Fourier spectrum, see Fig. 5.5
- Estimate the noise PDF → capture a set of “flat images” to study the shape of the histogram, see Fig. 5.6

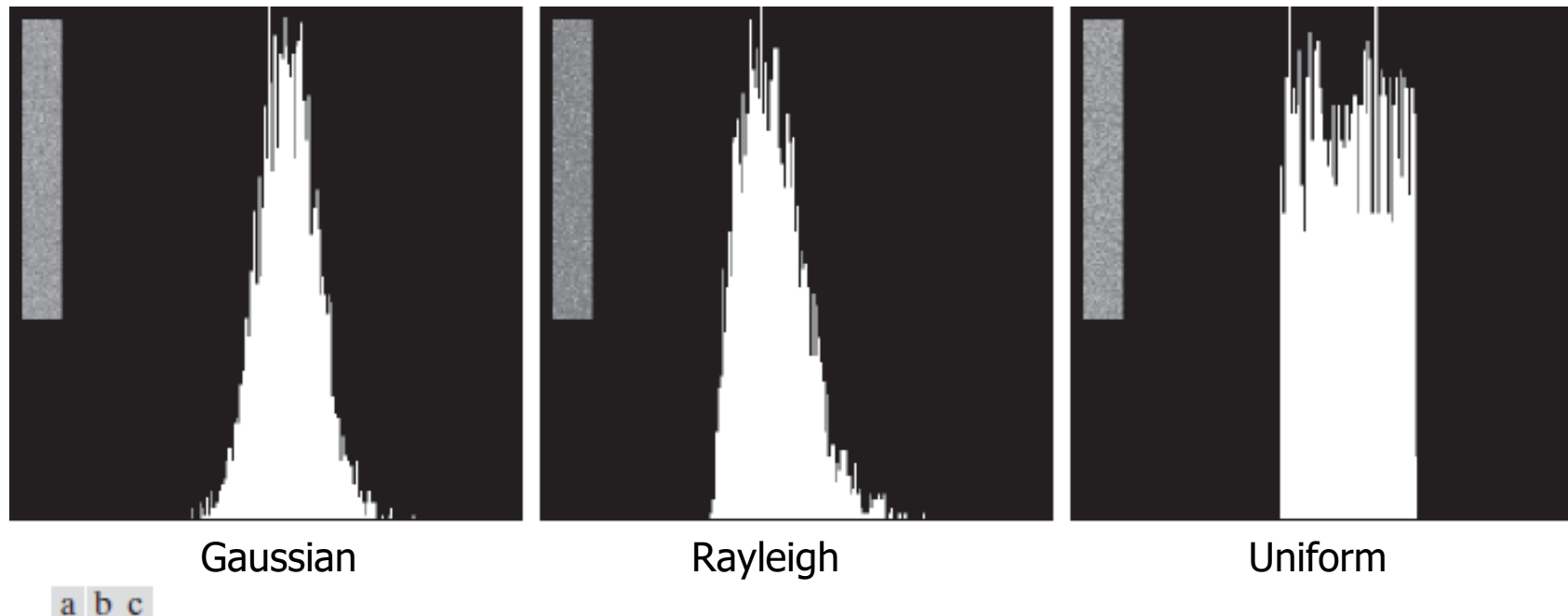


FIGURE 5.6 Histograms computed using small strips (shown as inserts) from (a) the Gaussian, (b) the Rayleigh, and (c) the uniform noisy images in Fig. 5.4.

Estimation of Noise Parameters (2)

1. Denote the subimage under consideration by S .
2. Compute $p_s(z_i)$, $i = 0, 1, \dots, L-1$, representing the probability of the intensities of pixels in S .
3. Compute the mean and variance of the pixels in S :

$$\bar{z} = \sum_{i=0}^{L-1} z_i p_s(z_i)$$

and

$$\sigma^2 = \sum_{i=0}^{L-1} (z_i - \bar{z})^2 p_s(z_i).$$

4. Use the resulting \bar{z} and σ^2 to solve for a and b of the noise model.

p7~p12那些式子的a,b参数

Restoration by Spatial Filtering

- Consider an image degraded only by additive noise

$$g(x, y) = f(x, y) + \eta(x, y)$$

(noise)

or

$$G(u, v) = F(u, v) + N(u, v)$$

where the noise term is generally unknown.

- For periodic noise, if $N(u, v)$ can be obtained from $G(u, v)$, we can subtract $N(u, v)$ from $G(u, v)$ to obtain $F(u, v)$.
- In general, we obtain an estimate of $f(x, y)$ by using the spatial filtering discussed in Chap. 3

Spatial Filtering: Arithmetic Mean Filter

Let S_{xy} represent the set of pixels in a rectangle subimage of size $m \times n$ and with center at (x, y) .

Arithmetic mean filter

$$f(x, y) = \frac{1}{mn} \sum_{(r, c) \in S_{xy}} g(r, c)$$

Spatial Filtering: Geometric Mean Filter

Geometric mean filter

$$f(x, y) = \left[\prod_{(r,c) \in S_{xy}} g(r, c) \right]^{\frac{1}{mn}}$$

- Smoothing capability comparable to arithmetic mean filter
- Preserve image detail better than arithmetic mean filter



Spatial Filtering: Harmonic Mean Filter

Harmonic mean filter

$$\hat{f}(x, y) = \frac{mn}{\sum_{(r,c) \in S_{xy}} \frac{1}{g(r, c)}}$$

- Works well for **salt noise** 
- Also works for other types of noise like Gaussian noise 
- Fails for pepper noise 

Spatial Filtering: Contraharmonic Mean Filter

Contraharmonic mean filter

$$f(x, y) = \frac{\sum_{(r,c) \in S_{xy}} g(r, c)^{Q+1}}{\sum_{(r,c) \in S_{xy}} g(r, c)^Q}$$

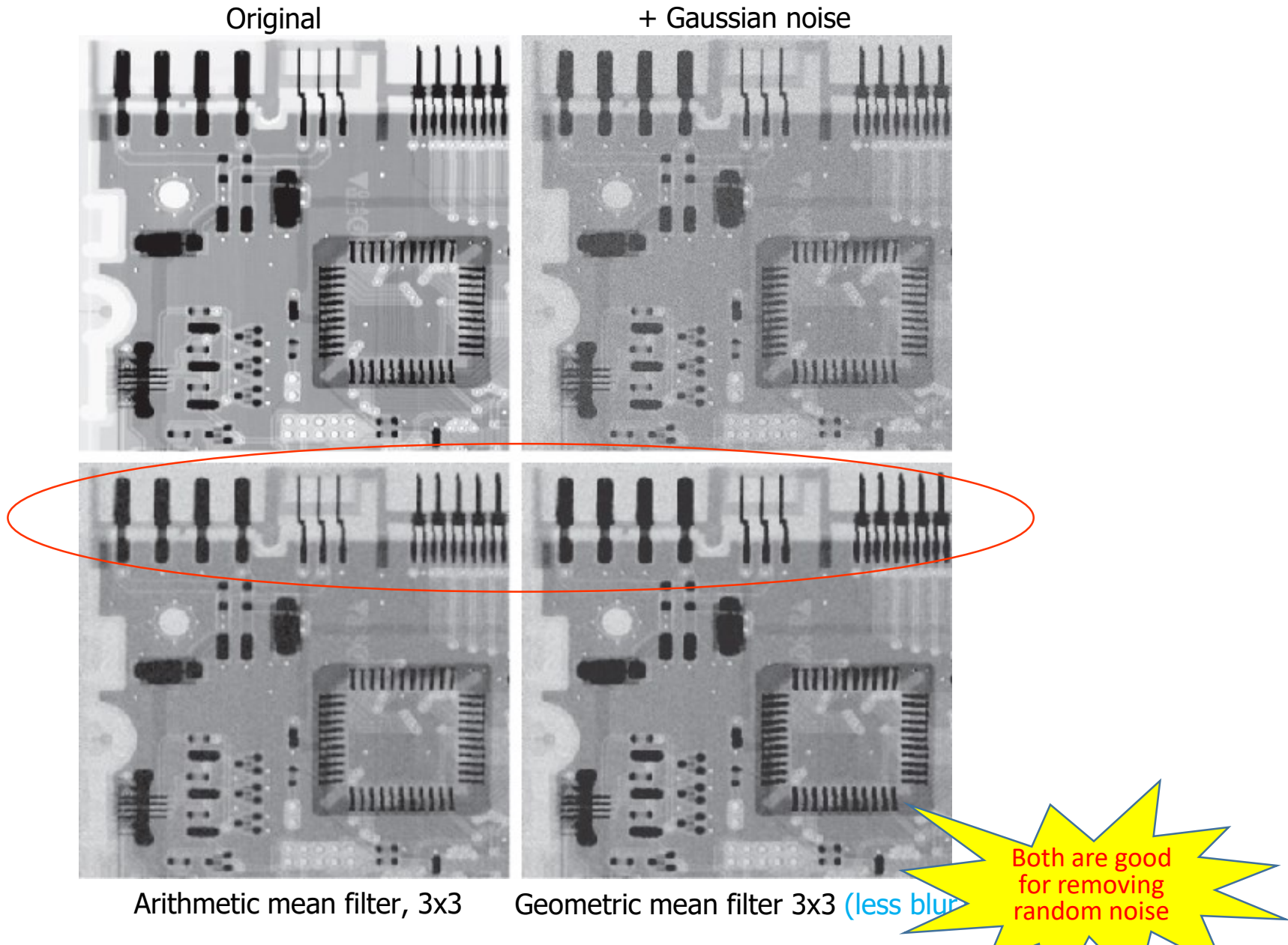
- Q: order of the filter
- Well suited for salt-and-pepper noise
 - Q>0 for pepper noise
 - Q<0 for salt noise

若顛倒會變 p27 那樣
- But cannot remove both at the same time
- Q=0, arithmetic mean filter
- Q=-1, harmonic mean filter

Spatial Filtering: Example (1)

a
b
c
d

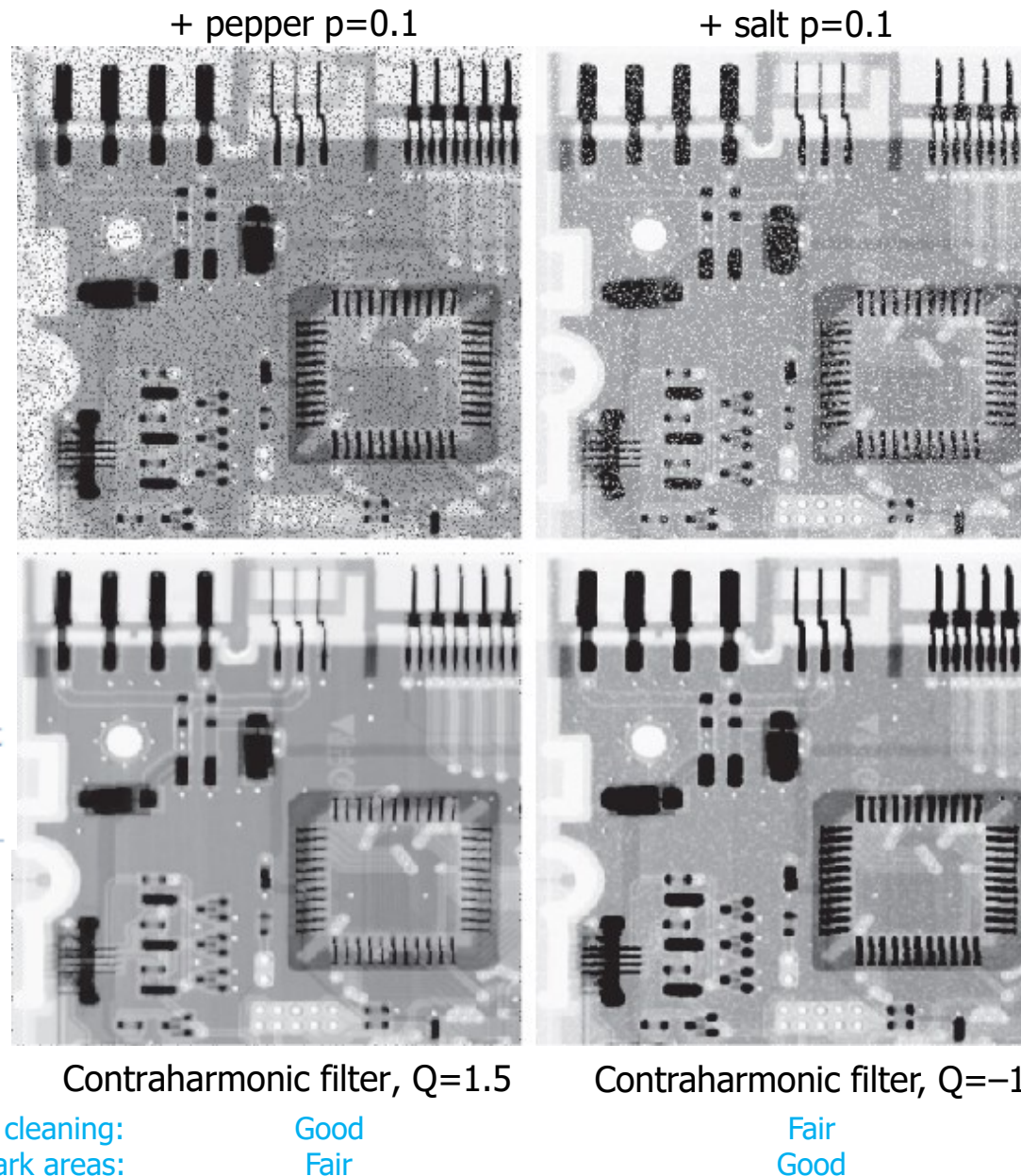
FIGURE 5.7
(a) X-ray image of circuit board.
(b) Image corrupted by additive Gaussian noise. (c) Result of filtering with an arithmetic mean filter of size 3×3 . (d) Result of filtering with a geometric mean filter of the same size. (Original image courtesy of Mr. Joseph E. Pascente, Lixi, Inc.)



Spatial Filtering: Example (2)

a
b
c
d

FIGURE 5.8
(a) Image corrupted by pepper noise with a probability of 0.1. (b) Image corrupted by salt noise with the same probability.
(c) Result of filtering (a) with a 3×3 contra-harmonic filter $Q = 1.5$. (d) Result of filtering (b) with $Q = -1.5$.



Good for removing
impulse noise

Spatial Filtering: Example (3)

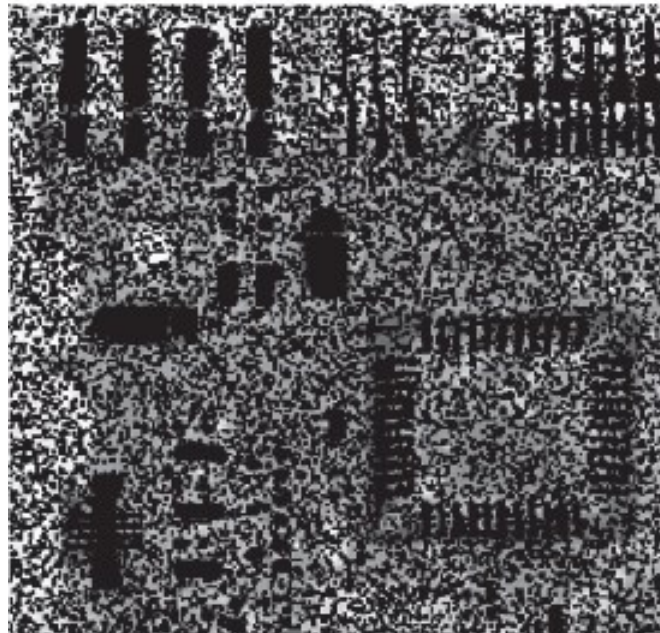
a b

FIGURE 5.9

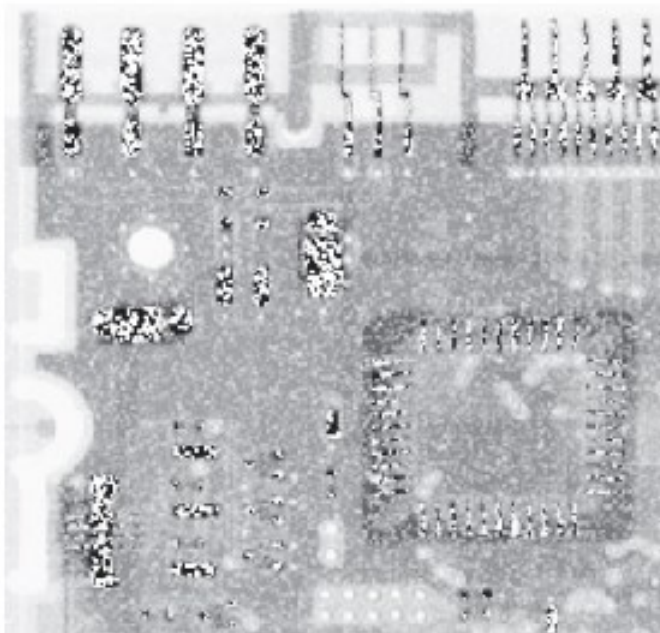
Results of selecting the wrong sign in contraharmonic filtering.

- (a) Result of filtering Fig. 5.8(a) with a contraharmonic filter of size 3×3 and $Q = -1.5$.
(b) Result of filtering Fig. 5.8(b) using $Q = 1.5$.

pepper

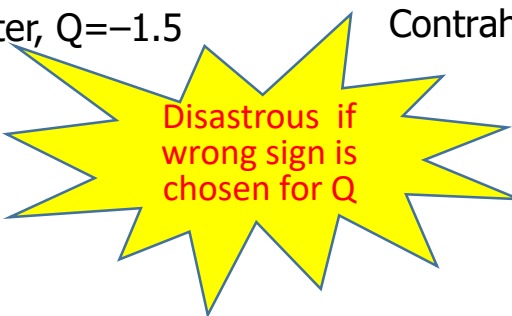


salt



Contraharmonic filter, $Q = -1.5$

Contraharmonic filter, $Q = 1.5$



p 24

Spatial Filtering: Order-Statistic Filters (1)

Median filter $f(x, y) = \underset{(r, c) \in S_{xy}}{\text{median}} \{g(r, c)\}$

Max filter $f(x, y) = \underset{(r, c) \in S_{xy}}{\max} \{g(r, c)\}$

Min filter $f(x, y) = \underset{(r, c) \in S_{xy}}{\min} \{g(r, c)\}$

Midpoint filter $f(x, y) = \frac{1}{2} \left[\underset{(r, c) \in S_{xy}}{\max} \{g(r, c)\} + \underset{(r, c) \in S_{xy}}{\min} \{g(r, c)\} \right]$

Spatial Filtering: Order-Statistic Filters (2)

Alpha-trimmed mean filter

- Remove the $d/2$ lowest values and $d/2$ highest values.
- Denote the remaining $mn - d$ pixels in $S_{x,y}$ by $g_R(x,y)$.
- Compute

$$f(x,y) = \frac{1}{mn-d} \sum_{(r,c) \in S_{xy}} \{g_R(r,c)\}$$

where

$$0 \leq d \leq mn - 1.$$

- $d = 0$, arithmetic mean filter
- $d = mn - 1$, median filter

WHY? ; $mn - d = mn - (mn - 1) = 1$

Repeated Applications of Median Filtering

a b
c d

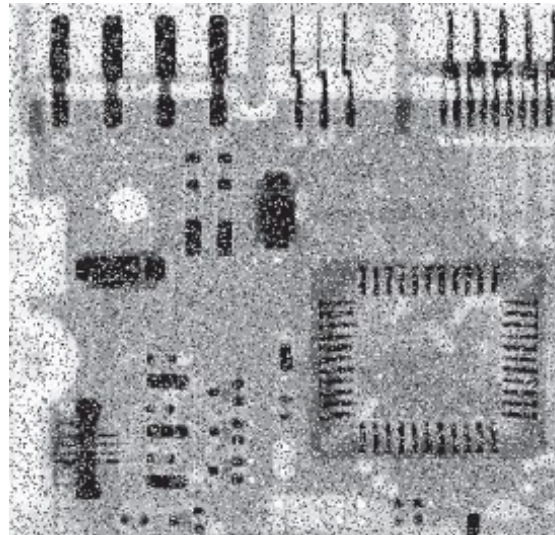
FIGURE 5.10

(a) Image corrupted by salt-and-pepper noise with probabilities $P_s = P_p = 0.1$.

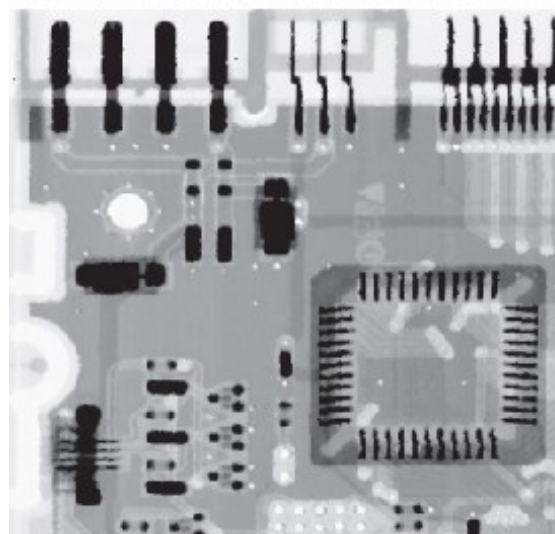
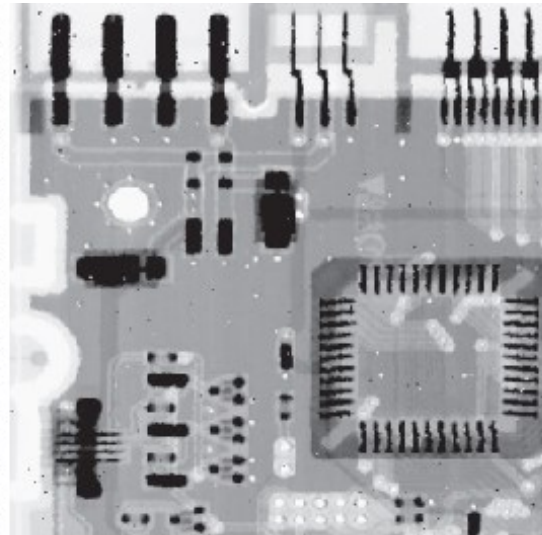
(b) Result of one pass with a median filter of size 3×3 . (c) Result of processing (b) with this filter.

(d) Result of processing (c) with the same filter.

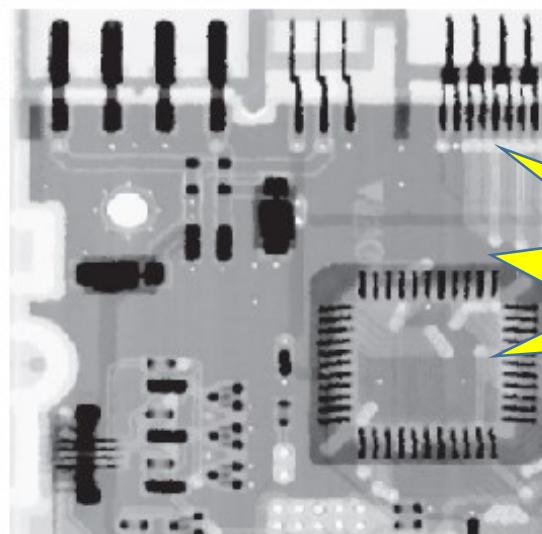
+ salt-and-pepper, $p=0.1$



first pass median filtering, 3×3



second pass



third pass

CAUTION

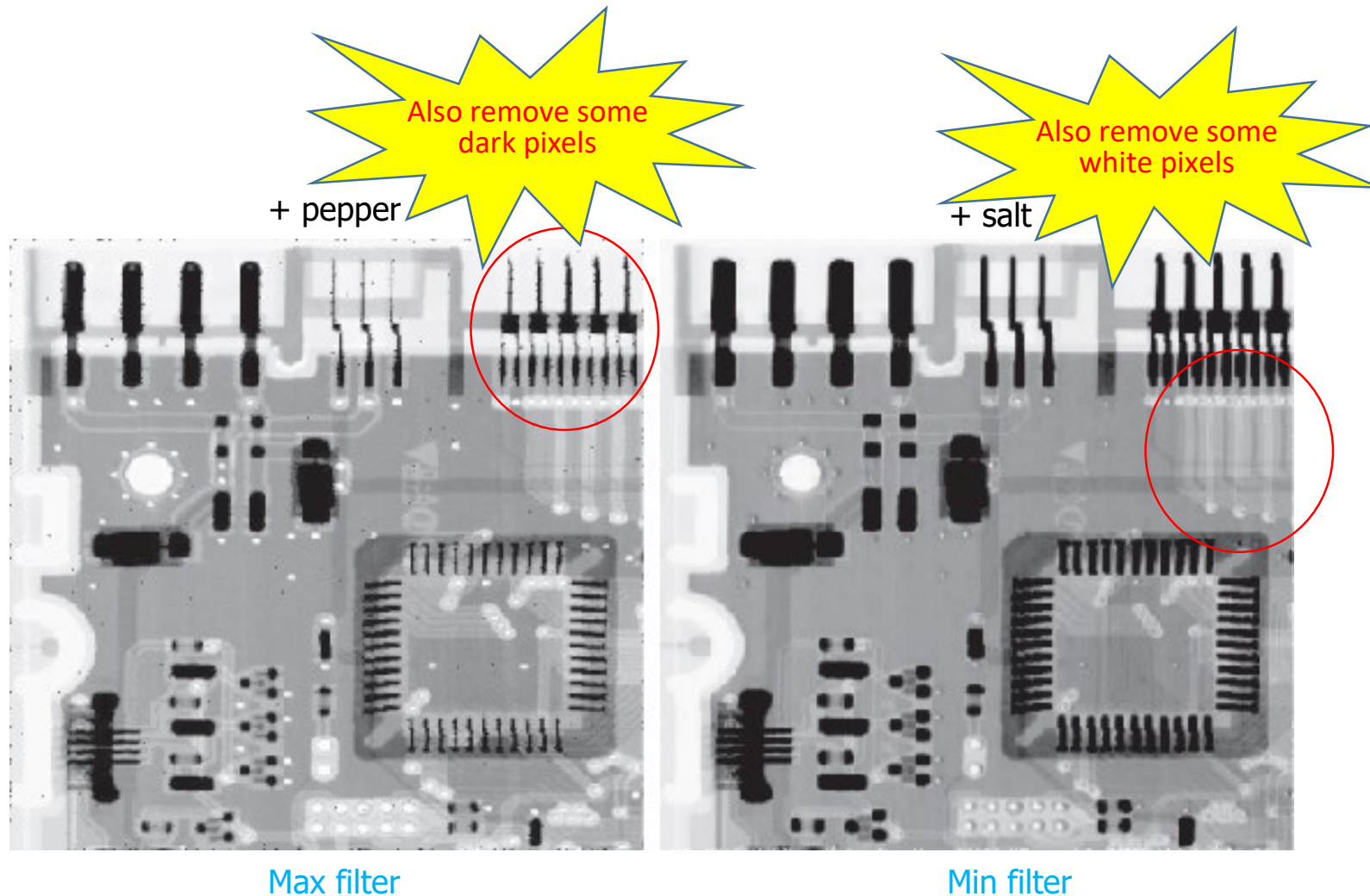
Good for impulse noise. But repeated median filtering may blur the image.

As a rule of thumb, the median filter works well when P_s and P_p are less than 0.2.

Result of Max and Min Filters

a b

FIGURE 5.11
(a) Result of filtering Fig. 5.8(a) with a max filter of size 3×3 .
(b) Result of filtering Fig. 5.8(b) with a min filter of the same size.



Spatial Filtering: Example

a	b
c	d
e	f

FIGURE 5.12

(a) Image corrupted by additive uniform noise. (b) Image additionally corrupted by additive salt-and-pepper noise.

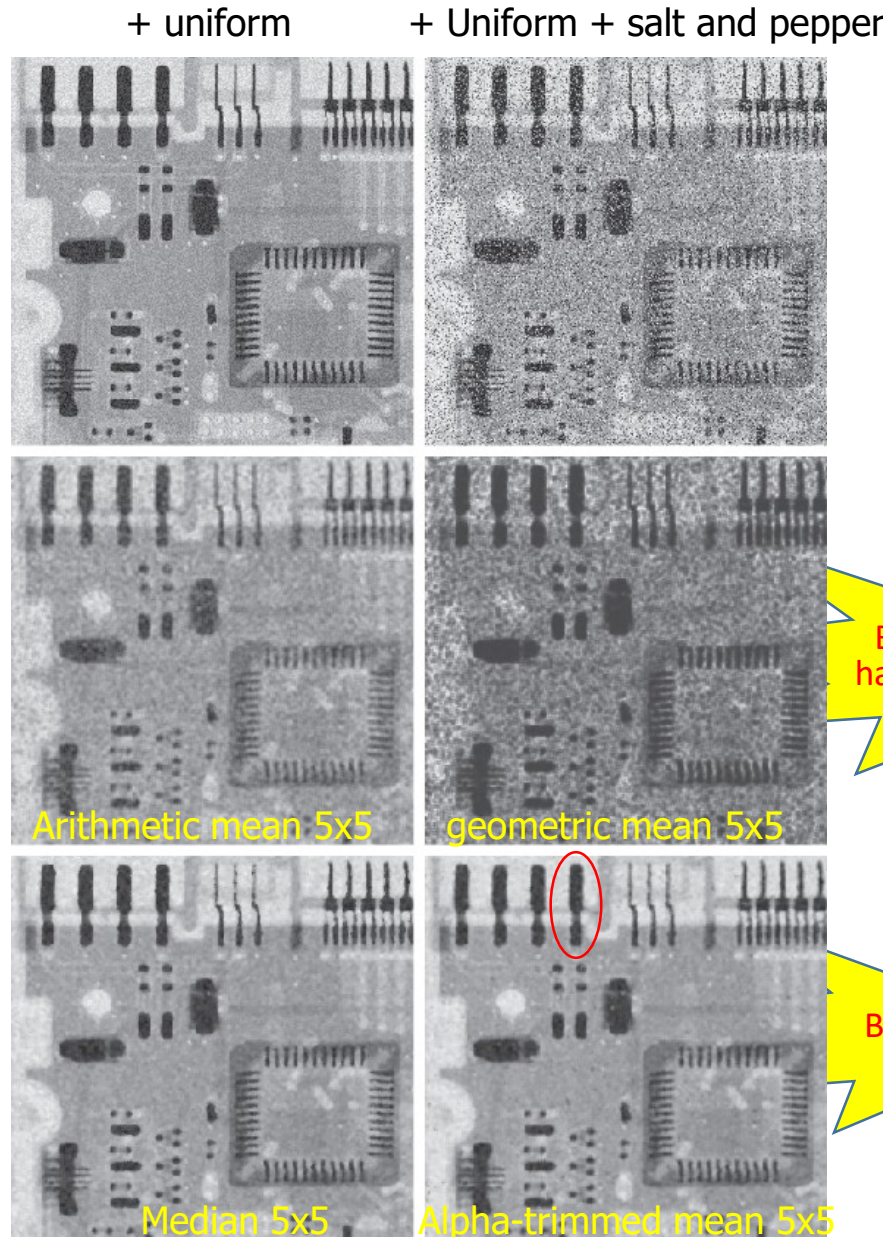
(c)-(f) Image (b) filtered with a

(c) arithmetic mean filter;

(d) geometric mean filter;

(e) median filter;

(f) alpha-trimmed mean filter, with $d = 6$.



Adaptive Filters

- Change behavior based on statistical characteristics of the image inside the $m \times n$ filter region defined by $S_{x,y}$
- Superior to other spatial filters discussed so far
- Price: increased complexity
- The response of the filter is based on four quantities:
 - $g(x, y)$: the value of the noisy image at (x, y)
 - σ_η^2 : the variance of the noise
 - $\bar{z}_{S_{xy}}$: the local mean of the pixels in S_{xy}
 - $\sigma_{S_{xy}}^2$: the local variance of the pixels in S_{xy}



Location dependent

Adaptive Local Noise Reduction Filter

Desired behavior of the filter:

- If $\sigma_\eta^2 = 0$, the filter should return simply the value of $g(x, y)$ Zero noise => $g(x,y) = f(x,y)$
- If $\sigma_{S_{xy}}^2$ is high relative to σ_η^2 , the filter should return a value close to $g(x, y)$ Want to preserve edges, which has a high local variance.
- If $\sigma_{S_{xy}}^2 \approx \sigma_\eta^2$, the filter returns the arithmetic mean value of the pixels in S_{xy} when local image = overall image, we reduce the noise by averaging.

Adaptive filter

$$\widehat{f}(x, y) = g(x, y) - \frac{\sigma_\eta^2}{\sigma_{S_{xy}}^2} [g(x, y) - \bar{z}_{S_{(x,y)}}]$$

Known a priori

Implicit assumption: $\sigma_\eta^2 < \sigma_{S_{xy}}^2 \Leftarrow$ should be checked



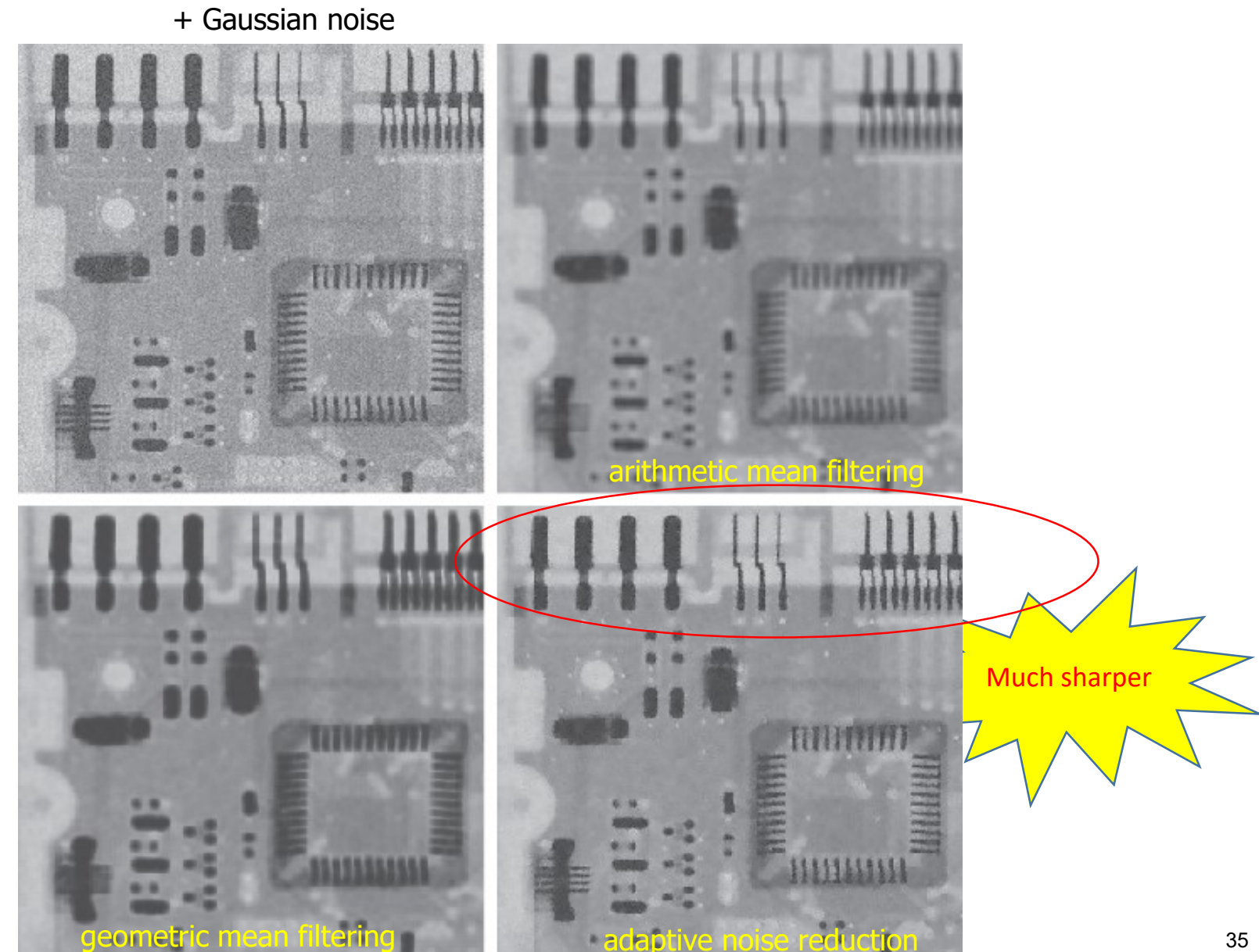
這個是前提

Result of Adaptive Noise Reduction

a | b
c | d

FIGURE 5.13

- (a) Image corrupted by additive Gaussian noise of zero mean and a variance of 1000.
(b) Result of arithmetic mean filtering 7×7
(c) Result of geometric mean filtering. 7×7
(d) Result of adaptive noise-reduction filtering. All filters used were of size 7×7 .



Adaptive Median Filters (1)

Objectives:

- Remove salt-and-pepper (impulse) noise
- Smooth non-impulsive noise in the meantime
- Reduce distortion such as excessive thinning or thickening of object boundaries

Features:

- Can handle noise with probability larger than 0.2
- Preserve detail while smoothing non-impulse noise
- Change the size of S_{xy} during filtering

Notations:

z_{\min} = minimum intensity value in S_{xy}

z_{\max} = maximum intensity value in S_{xy}

z_{med} = median intensity value in S_{xy}

z_{xy} = intensity value at (x, y)

S_{\max} = maximum allowed size of S_{xy}

↳ increase window大小

Adaptive Median Filters (2)

Has two processing levels at each pixel $I(x, y)$:

Level A:

{ If $z_{\min} < z_{\text{med}} < z_{\max}$, go to Level B

Else increase the size of $S_{x,y}$

{ If $S_{x,y} \leq S_{\max}$, repeat Level A

Else output z_{med}

Level B:

If $z_{\min} < z_{xy} < z_{\max}$, output z_{xy}

Else output z_{med}

The median filter output
is not an impulse

→ 不是 salt / pepper

→ 它是 z_{med} 是 salt / pepper

Determine if z_{med} is
an impulse (salt or
pepper)

The pixel is not
an impulse

→ 它不是被 salt pepper 污染到

Spatial Filtering: Example (8)

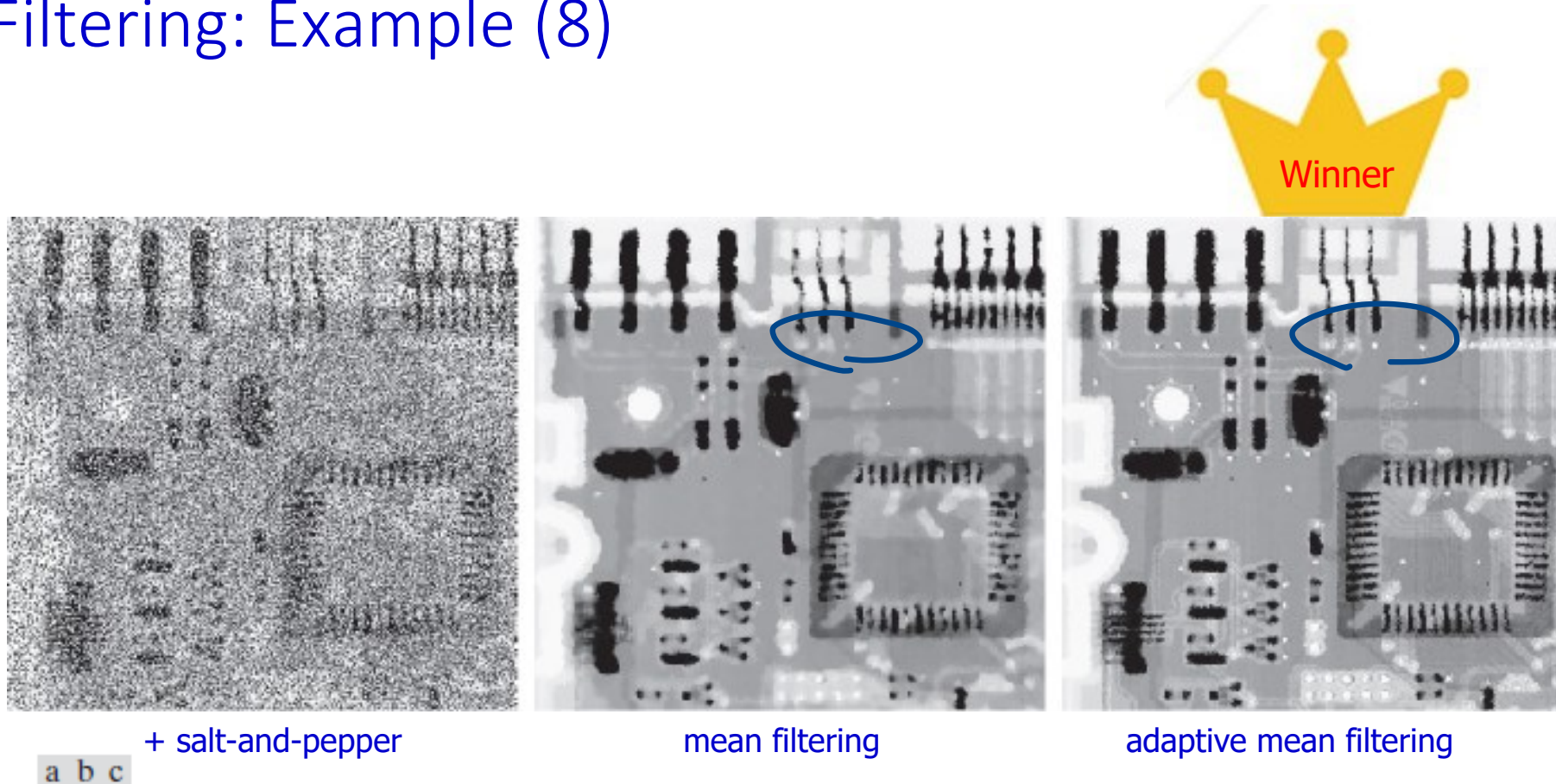


FIGURE 5.14 (a) Image corrupted by salt-and-pepper noise with probabilities $P_s = P_p = 0.25$. (b) Result of filtering with a 7×7 median filter. (c) Result of adaptive median filtering with $S_{\max} = 7$.

Frequency Domain Periodic Noise Reduction

Observation

Periodic noise appears as concentrated **bursts** in the Fourier transform, at locations corresponding to the frequencies of the periodic noise

Approach: Use a selective filter to isolate the noise

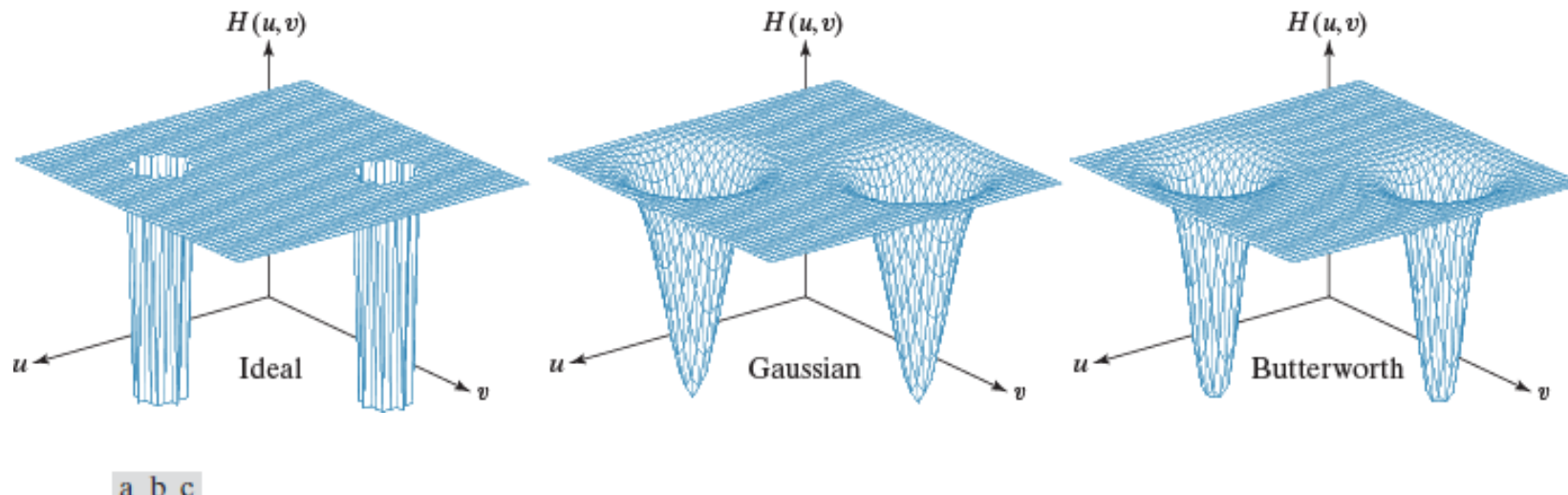


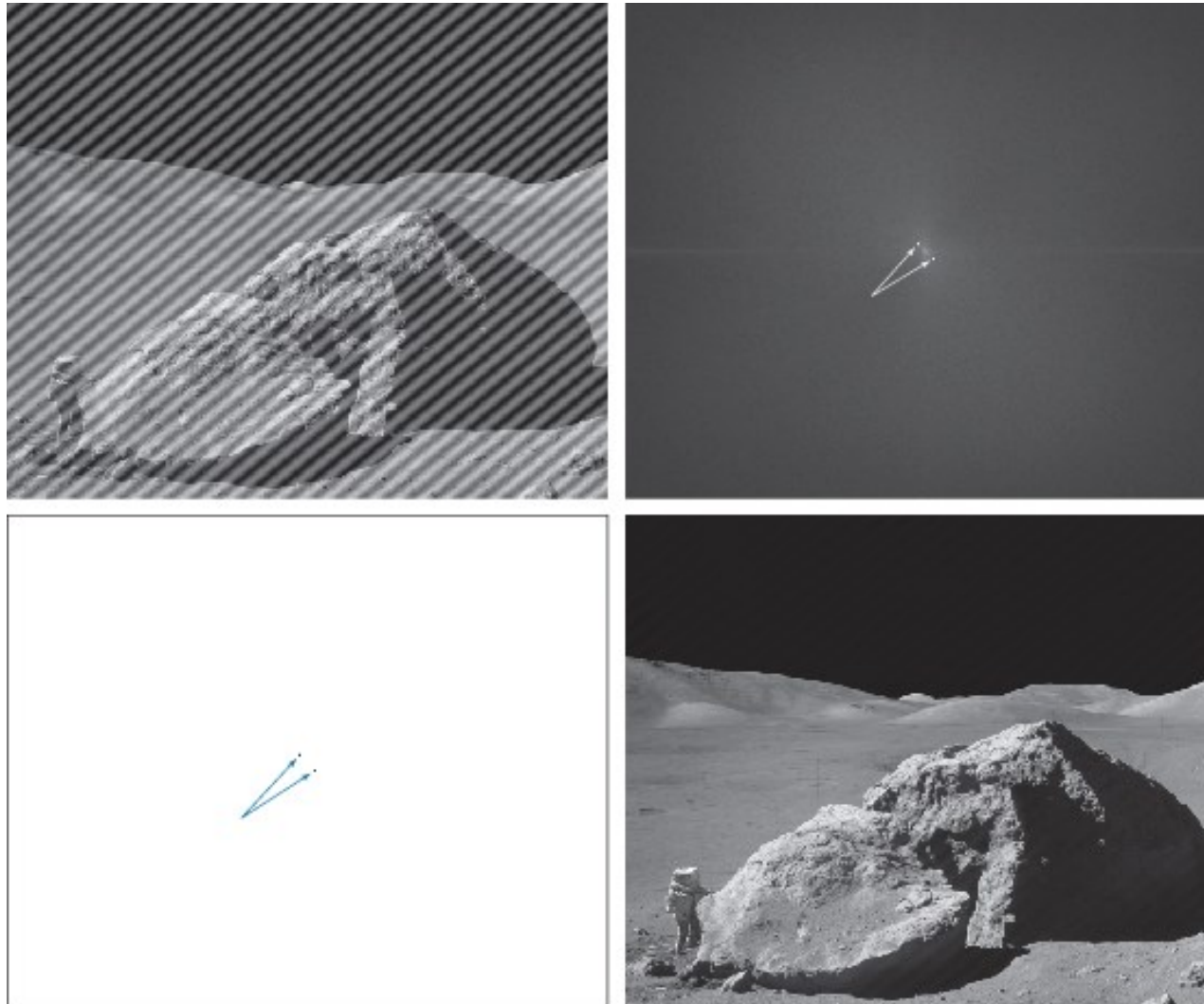
FIGURE 5.15 Perspective plots of (a) ideal, (b) Gaussian, and (c) Butterworth notch reject filter transfer functions.

Frequency Domain Periodic Noise Reduction

a
b
c
d

FIGURE 5.16

- (a) Image corrupted by sinusoidal interference.
(b) Spectrum showing the bursts of energy caused by the interference. (The bursts were enlarged for display purposes.)
(c) Notch filter (the radius of the circles is 2 pixels) used to eliminate the energy bursts. (The thin borders are not part of the data.)
(d) Result of notch reject filtering. (Original image courtesy of NASA.)



Frequency Domain Periodic Noise Reduction

FIGURE 5.17
Sinusoidal
pattern extracted
from the DFT
of Fig. 5.16(a)
using a notch pass
filter.

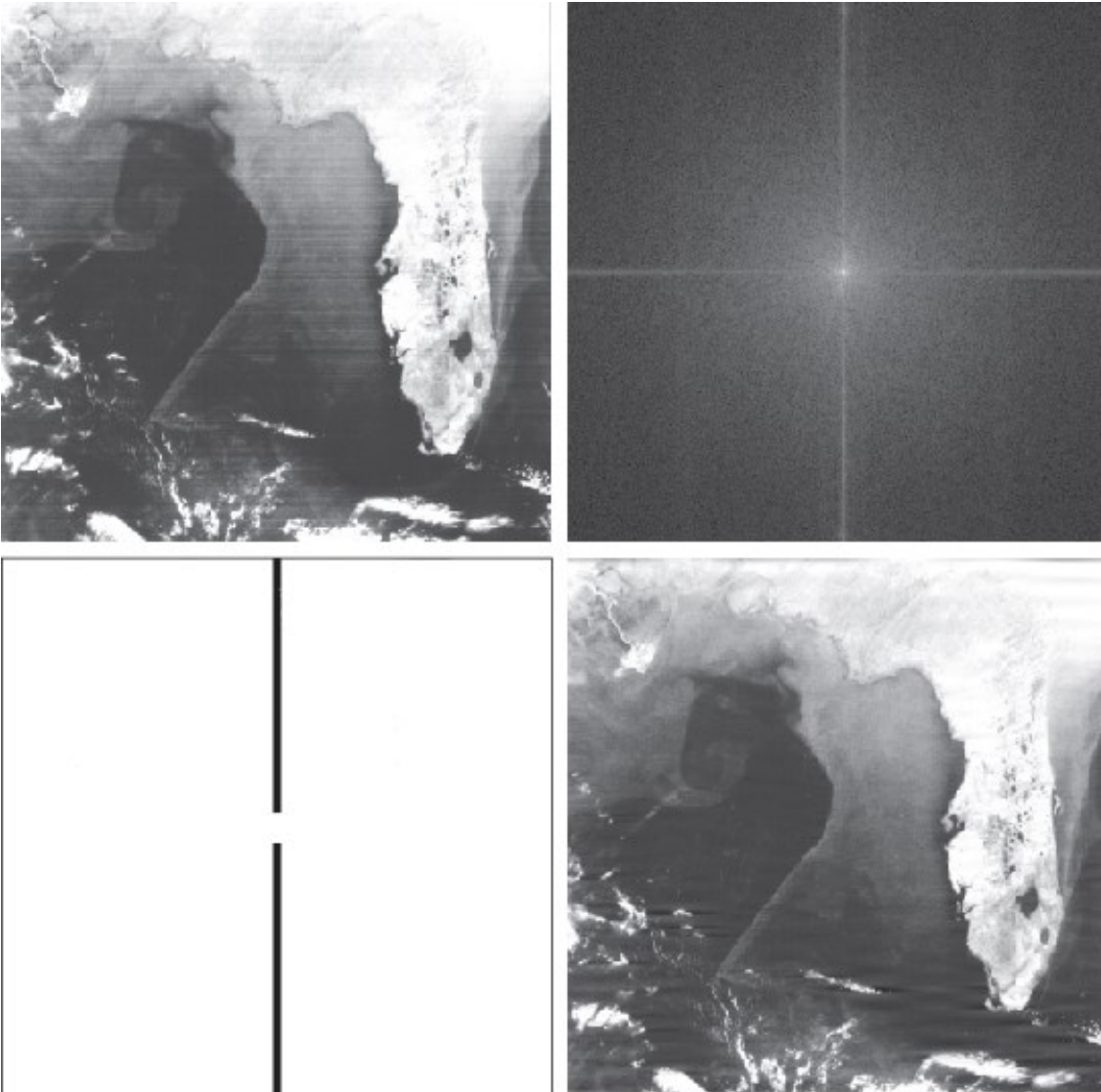


Frequency Domain Periodic Noise Reduction

a b
c d

FIGURE 5.18

(a) Satellite image of Florida and the Gulf of Mexico. (Note horizontal sensor scan lines.)
(b) Spectrum of (a). (c) Notch reject filter transfer function. (The thin black border is not part of the data.) (d) Filtered image. (Original image courtesy of NOAA.)



Frequency Domain Periodic Noise Reduction

FIGURE 5.19
Noise pattern
extracted from
Fig. 5.18(a) by
notch pass
filtering.

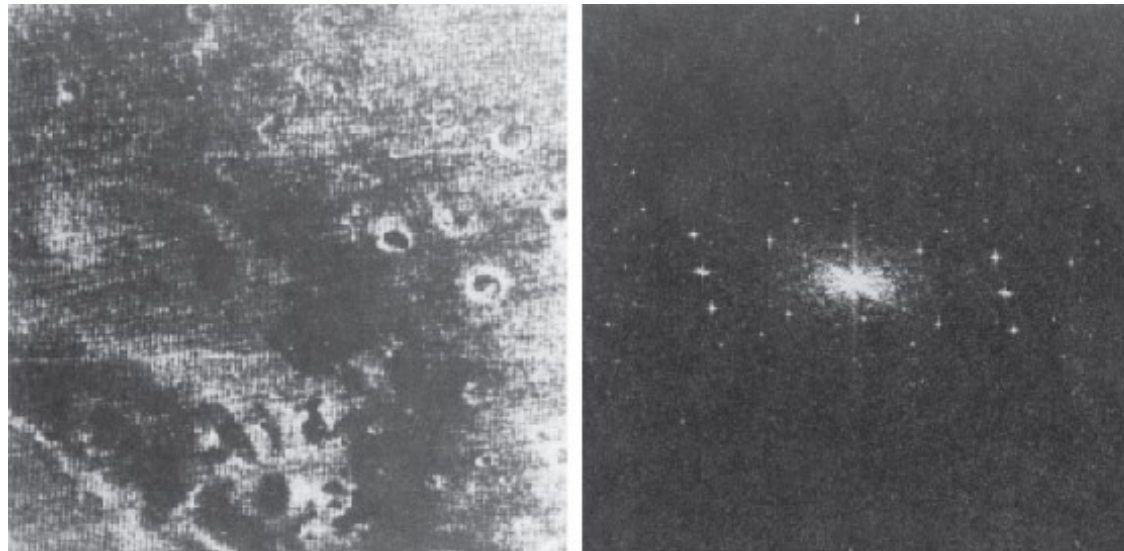


Frequency Domain Periodic Noise Reduction

a b

FIGURE 5.20

(a) Image of the Martian terrain taken by Mariner 6.
(b) Fourier spectrum showing periodic interference.
(Courtesy of NASA.)



- Several interference components are present, the heuristic specifications of filter transfer functions discussed in the preceding sections are not always acceptable because they remove much image information
- The interference components are not single-frequency bursts; they tend to have **broad skirts** that carry information about the interference pattern and the skirts are not always easily detectable.

Optimum Notch Filtering

- Naïve notch filters may remove too much image information when multiple severe interference components (not necessarily single-frequency bursts) are present.
- The method discussed next is optimum, in the sense that it minimizes local variances of the restored estimate $\hat{f}(x, y)$.
- Steps:
 1. Extract the principal contributions of the interference patterns
 2. Subtract a variable, weighted portion of the pattern from the corrupted image

Optimum Notch Filtering: Step 1

- ❑ Place a notch pass filter at the location of each spike.

$$N(u, v) = H_{NP}(u, v)G(u, v)$$

NP: notch pass

$$\eta(x, y) = \mathcal{I}^{-1} \{ H_{NP}(u, v)G(u, v) \}$$

- ❑ It requires considerable judgement about the interference spike, normally done **interactively**.
- ❑ In practice, we can only obtain an approximation of the true noise pattern.

Optimum Notch Filtering: Step 2 (1)

- Minimize the effect of incomplete components not present in the estimate of $\eta(x, y)$ by subtracting from $g(x, y)$ a weighted portion of $\eta(x, y)$ to obtain an estimate of $f(x, y)$:

$$\hat{f}(x, y) = g(x, y) - w(x, y)\eta(x, y)$$

- Select $w(x, y)$ so that the variance of $\hat{f}(x, y)$ is minimized over a specified neighborhood of every point (x, y) . Compute the local variance of $\hat{f}(x, y)$ by

$$\sigma^2(x, y) = \frac{1}{mn} \sum_{(r, c) \in S_{xy}} \left[\hat{f}(r, c) - \bar{\hat{f}}(x, y) \right]^2$$

$$\bar{\hat{f}}(x, y) = \frac{1}{mn} \sum_{(r, c) \in S_{xy}} \hat{f}(r, c)$$

Optimum Notch Filtering: Step 2 (2)

$$\sigma^2(x, y) = \frac{1}{mn} \sum_{(r, c) \in S_{xy}} \left\{ [g(r, c) - w(r, c)\eta(r, c)] - [\bar{g} - \bar{w}\bar{\eta}] \right\}^2$$

Assume w is approximately constant and is equal to the one at the center pixel

$$w(r, c) = w(x, y)$$

$$\bar{w} = w(x, y)$$

$$\bar{w}\bar{\eta} = w(x, y)\bar{\eta}$$

Therefore,

$$\sigma^2(x, y) = \frac{1}{mn} \sum_{(r, c) \in S_{xy}} \left\{ [g(r, c) - w(x, y)\eta(r, c)] - [\bar{g} - w(x, y)\bar{\eta}] \right\}^2$$

To minimize $\sigma^2(x, y)$, we solve $\frac{\partial \sigma^2(x, y)}{\partial w(x, y)} = 0$ for $w(x, y)$ and obtain

$$w(x, y) = \frac{\bar{g}(x, y)\bar{\eta}(x, y) - \bar{g}(x, y)\bar{\eta}(x, y)}{\bar{\eta}^2(x, y) - \bar{\eta}^2(x, y)}$$

where \bar{g} denotes the average value of g and $\bar{g}\bar{\eta}$ the average value of $g\eta$.

Denoising Using Optimum Notch Filtering

a b

FIGURE 5.20

(a) Image of the Martian terrain taken by Mariner 6.
(b) Fourier spectrum showing periodic interference.
(Courtesy of NASA.)



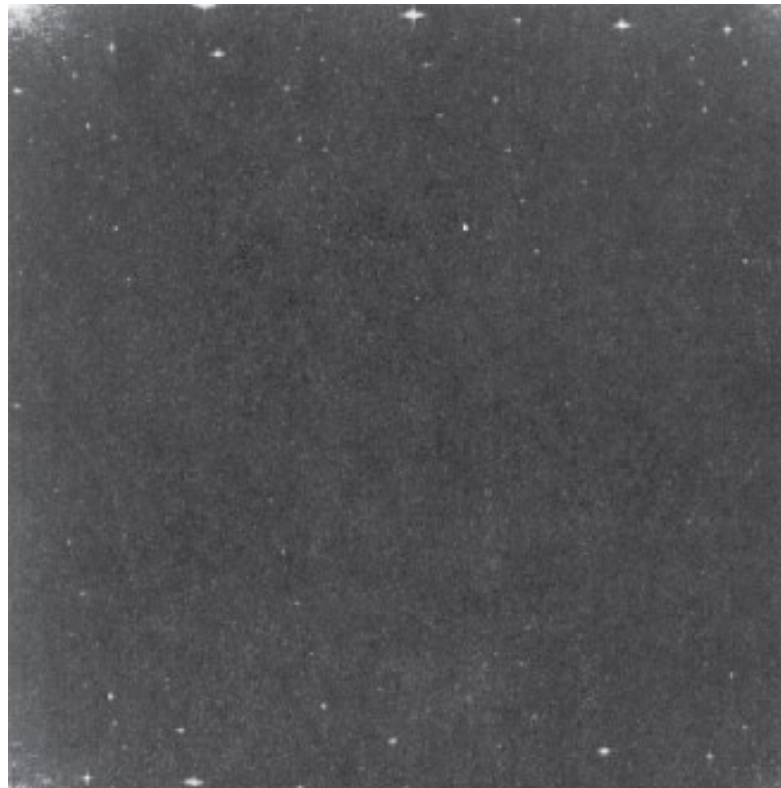
Semi-periodic interference



Star-like bursts

Denoising Using Optimum Notch Filtering

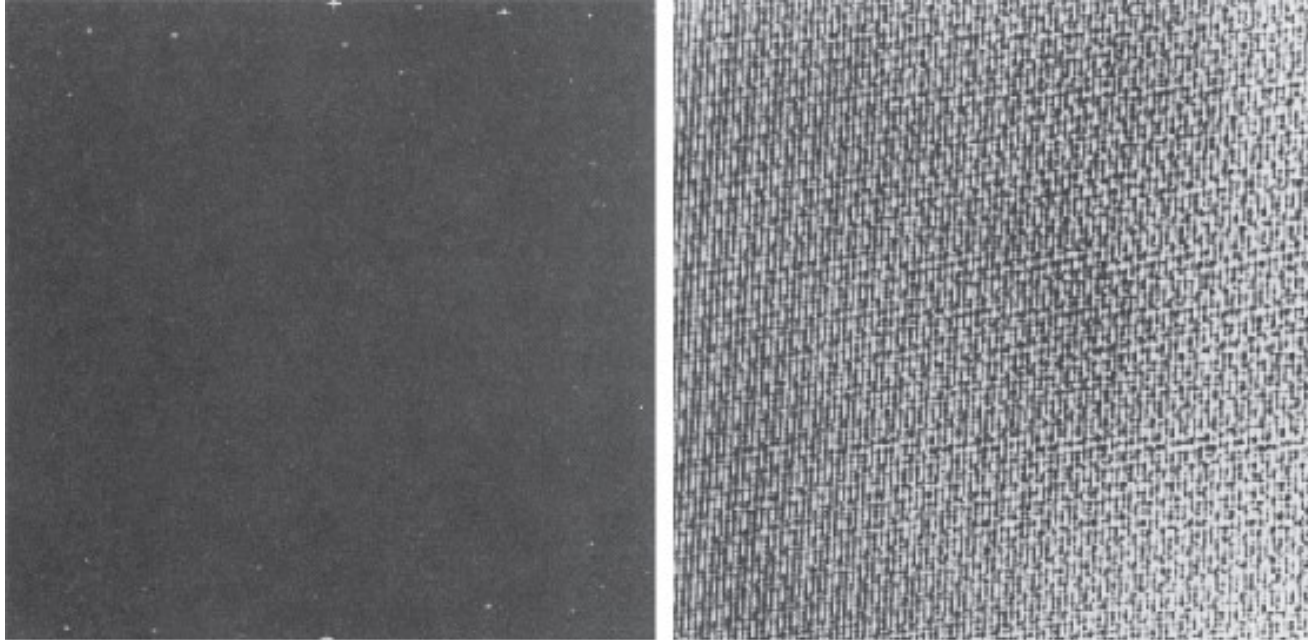
FIGURE 5.21
Uncentered
Fourier spectrum
of the image
in Fig. 5.20(a).
(Courtesy of
NASA.)



Denoising Using Optimum Notch Filtering

a b

FIGURE 5.22
(a) Fourier spectrum of $N(u,v)$,
and
(b) corresponding
spatial noise
interference
pattern, $\eta(x,y)$.
(Courtesy of
NASA.)



Spectral components associated
with the interference identified
by experts

$\eta(x,y)$

Denoising Using Optimum Notch Filtering

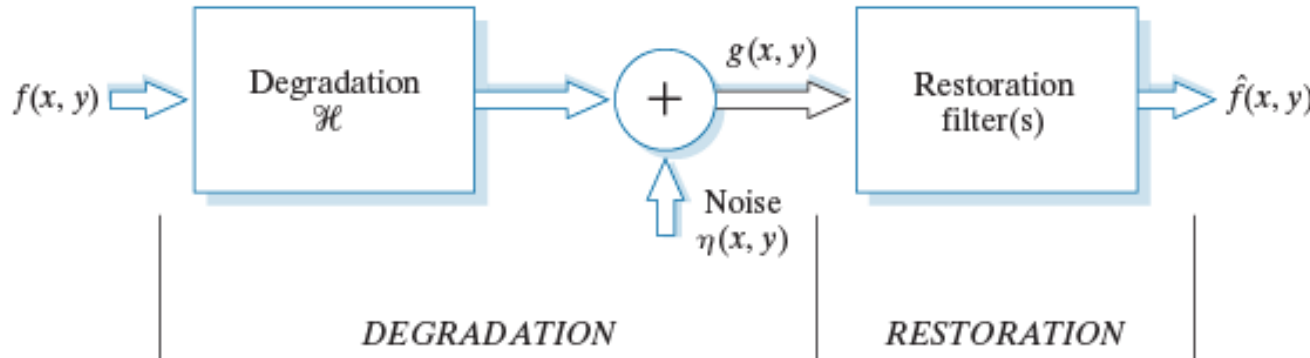


Original corrupted image



FIGURE 5.23
Restored image.
(Courtesy of
NASA.)

Linear, Position-Invariant Degradations



In the presence of additive noise, if H is linear and position invariant,

$$\begin{aligned} g(x, y) &= \int_{-\infty}^{\infty} \int_{-\infty}^{\infty} f(\alpha, \beta) h(x - \alpha, y - \beta) d\alpha d\beta + \eta(x, y) \\ &= h(x, y) * f(x, y) + \eta(x, y) \end{aligned}$$

f 和 h 的 convolution 加上 η

$$G(u, v) = H(u, v)F(u, v) + N(u, v)$$

在 freq. domain 是 Fourier 相乘

Estimating the Degradation Function

Three principal ways to estimate the degradation function:

1. By observation

From a subimage of strong content and its processed image, compute

$$H_s(u, v) = \frac{G_s(u, v)}{\hat{F}_s(u, v)}.$$

Our estimate of
the original image

2. By experimentation

From an impulse response and its intensity, compute

$$H(u, v) = \frac{G_s(u, v)}{A}.$$

3. By mathematical modeling



係這就是一個 impulse

a b

FIGURE 5.24
Estimating a
degradation by
impulse
characterization.
(a) An impulse of light (shown
magnified).
(b) Imaged (degraded)
impulse.

Image Blur due to Atmospheric Turbulence

Degradation model of atmospheric turbulence by Hufnagel and Stanley [64]

$$H(u, v) = e^{-k(u^2 + v^2)^{5/6}}$$

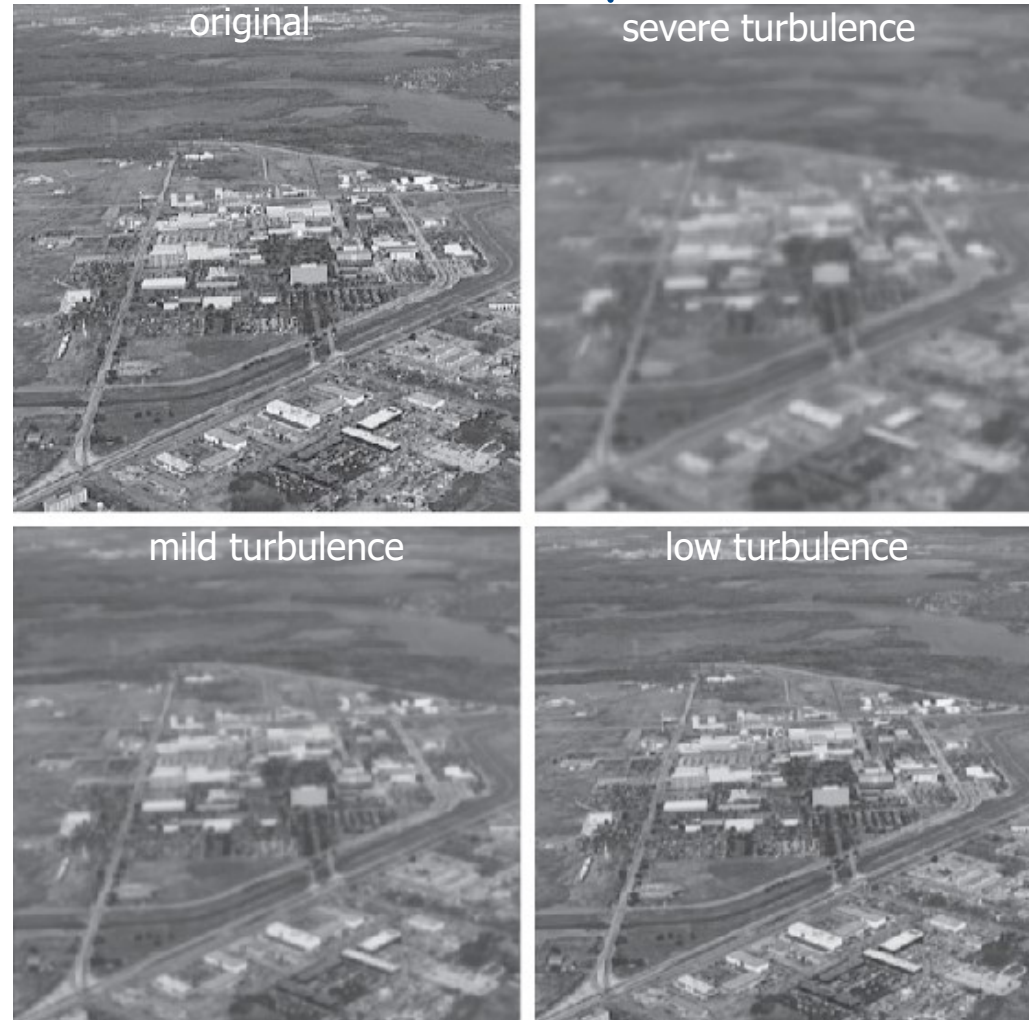
k : a constant whose value depends on the nature of the turbulence

a b
c d

FIGURE 5.25
Modeling turbulence.
(a) No visible turbulence.
(b) Severe turbulence.

(c) Mild turbulence.
(d) Low turbulence.

All images are of size 480×480 pixels.
(Original image courtesy of NASA.)



$K=0.0025$

$K=0.00025$

Motion Blur (1)

- Suppose that an image $f(x, y)$ undergoes planar motion and that the optical imaging process is perfect.
- Let $x_0(t)$ and $y_0(t)$ denote the time-varying components of motion in the x - and y -directions, respectively.
- Denote the duration of exposure by T .
- The blurred image $g(x, y)$ can be modeled by

$$g(x, y) = \int_0^T f[x - x_0(t), y - y_0(t)] dt$$

↳ “是累積光，∴用積分”

Motion Blur (2)

$$\begin{aligned} G(u, v) &= \int_{-\infty}^{\infty} \int_{-\infty}^{\infty} g(x, y) e^{-j2\pi(ux+vy)} dx dy \\ &= \int_{-\infty}^{\infty} \int_{-\infty}^{\infty} \left[\int_0^T f[x - x_0(t), y - y_0(t)] dt \right] e^{-j2\pi(ux+vy)} dx dy \\ &= \int_0^T \left[\int_{-\infty}^{\infty} \int_{-\infty}^{\infty} f[x - x_0(t), y - y_0(t)] e^{-j2\pi(ux+vy)} dx dy \right] dt \\ &= \int_0^T F(u, v) e^{-j2\pi[u x_0(t) + v y_0(t)]} dt \\ &= F(u, v) \underbrace{\int_0^T e^{-j2\pi[u x_0(t) + v y_0(t)]} dt}_{H(u, v)} \end{aligned}$$

又這個卷積對物也是類似的

Motion Blur (3)

$$H(u, v) = \int_0^T e^{-j2\pi[u x_0(t) + v y_0(t)]} dt$$

Uniform linear motion in the x -direction at a rate given by $x_0(t) = at / T$:

$$\begin{aligned} H(u, v) &= \int_0^T e^{-j2\pi u x_0(t)} dt \\ &= \int_0^T e^{-j2\pi u a t / T} dt \\ &= \frac{T}{\pi u a} \sin(\pi u a) e^{-j\pi u a} \end{aligned}$$

Motion Blur (4)

Uniform linear motion in x - and y -directions at a rate given by

$$x_0(t) = at/T \text{ and } y_0(t) = bt/T.$$

Then the degradation function becomes

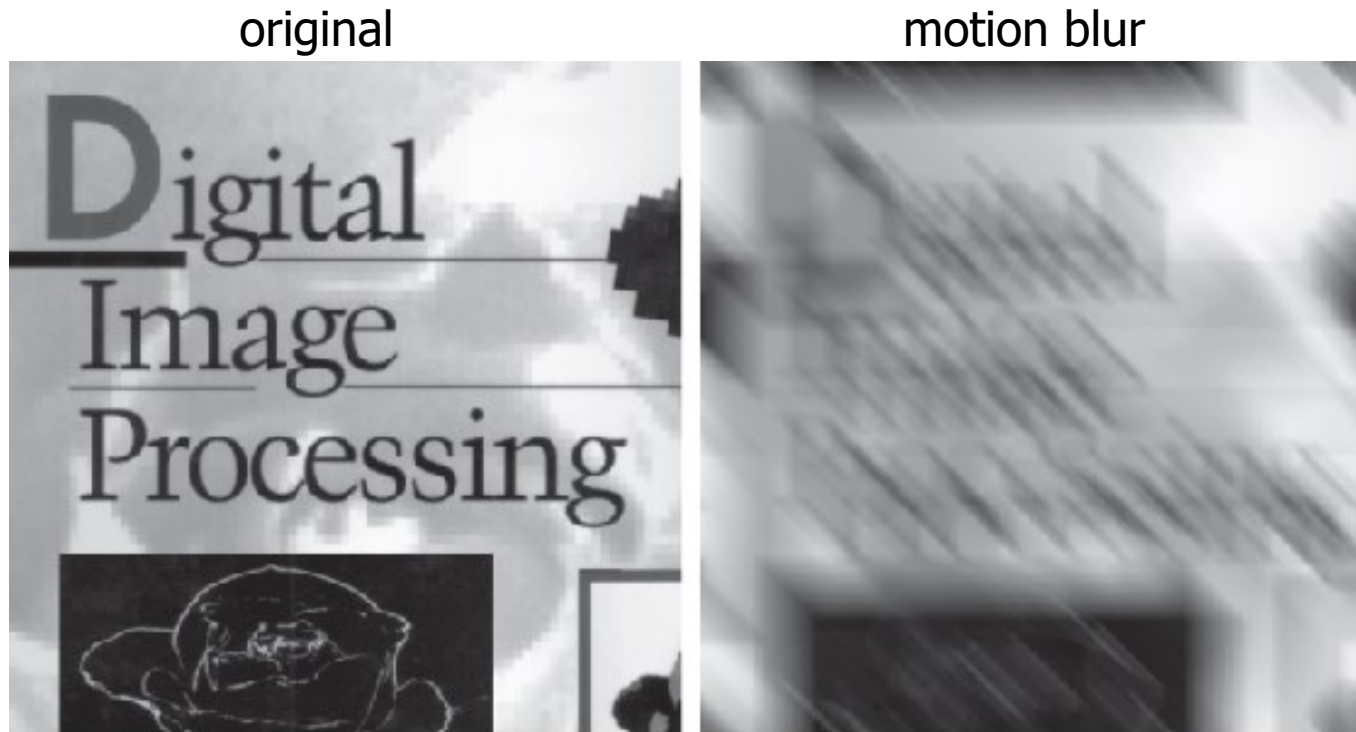
$$\begin{aligned} H(u, v) &= \int_0^T e^{-j2\pi[ux_0(t)+vy_0(t)]} dt \\ &= \int_0^T e^{-j2\pi[ua+vb]t/T} dt \\ &= \frac{T}{\pi(ua+vb)} \sin[\pi(ua+vb)] e^{-j\pi(ua+vb)} \end{aligned}$$

for rotation
motion by $H(u, v)$

Motion Blur

a b

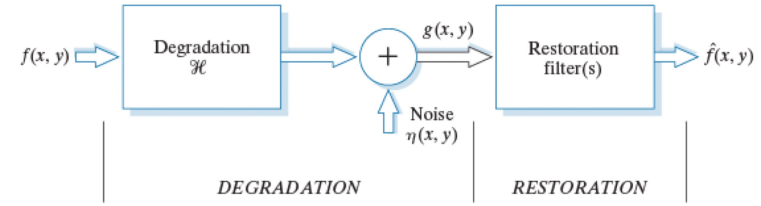
FIGURE 5.26
(a) Original
image. (b) Result
of blurring using
the function in
Eq. (5-77) with
 $a = b = 0.1$ and
 $T = 1$.



Inverse Filtering

The simplest approach to image restoration is to compute an estimate of the transform of the original image by

$$\begin{aligned}\hat{F}(u, v) &= \frac{G(u, v)}{H(u, v)} = \frac{F(u, v)H(u, v) + N(u, v)}{H(u, v)} \\ &= F(u, v) + \frac{N(u, v)}{H(u, v)}\end{aligned}$$



1. We can't exactly recover the image because $N(u, v)$ is not known.
2. If the degradation function has zero or very small values, then the ratio $N(u, v) / H(u, v)$ could easily dominate the estimate $\hat{F}(u, v)$.

$f(x, y) \rightarrow \text{degradation} \rightarrow \text{restoration} \rightarrow \text{原圖}$
 $H(x) \quad H^{-1}(x) \quad \text{但現在是有 noise}$

Inverse Filtering

EXAMPLE

Using the exact inverse of the degradation function

$$H(u, v) = e^{-k[(u-M/2)^2 + (v-N/2)^2]^{5/6}}$$

$$k = 0.0025, M = N = 480$$

to restore the image in Fig. 5.25(b). $H(u, v)$ is not zero because Gaussian functions have no zeros. Despite this, the degradation values become so small that the result of full inverse filtering is useless.

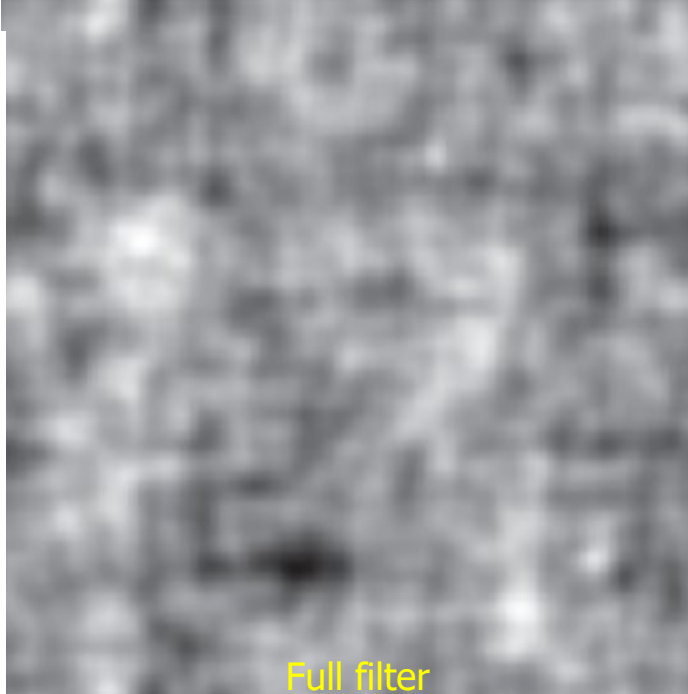
One approach is to get around the zero or small-value problem is to **limit the filter frequencies to values near the origin**.

This is done by applying a BLPF of order 10 to $N(u, v)/H(u, v)$.

a b
c d

FIGURE 5.27

Restoring
Fig. 5.25(b)
using Eq. (5-78).
(a) Result of using
the full filter.
(b) Result with H
cut off outside a
radius of 40.
(c) Result with H
cut off outside a
radius of 70.
(d) Result with H
cut off outside a
radius of 85.



Full filter



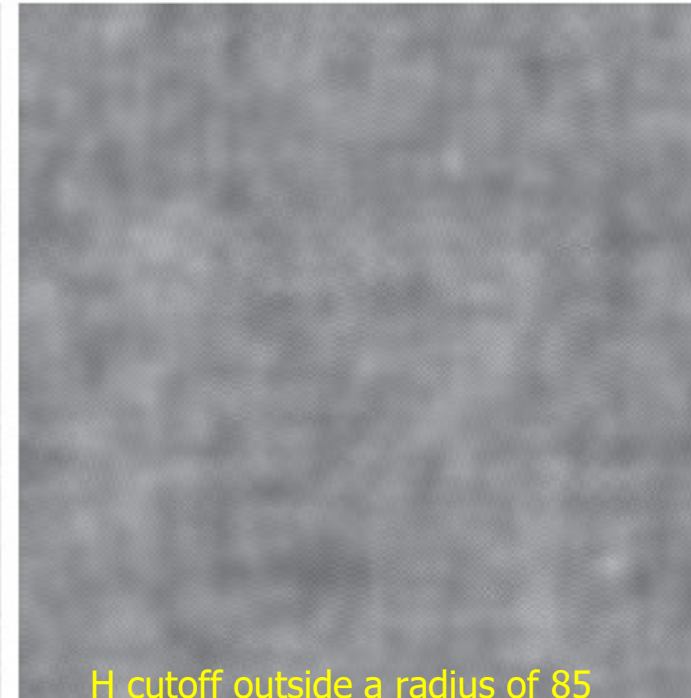
H cutoff outside a radius of 40

480 x 480 image

Cut off by a
Butterworth
LPF of order
10



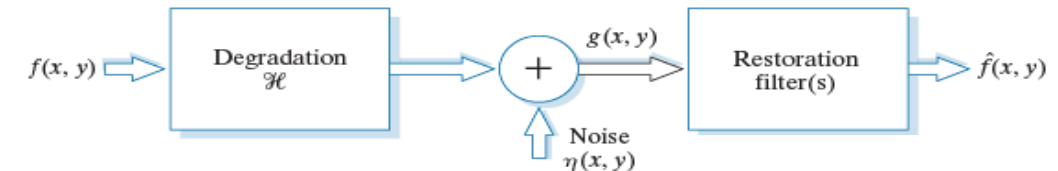
H cutoff outside a radius of 70



H cutoff outside a radius of 85

Minimum Mean Square Error (Wiener) Filtering

- **Norbert Wiener (1942)**



- **Objective:** In the presence of degradation and noise, find an estimate of the uncorrupted image such that the mean square error between them is minimized

$$e^2 = E\{(f - \hat{f})^2\} : \text{目標} \cdot \text{minimize } \text{这个 } e$$

假設
前提
under the following assumptions:

- 1) The noise and the image are uncorrelated
- 2) The noise or the image has zero mean
- 3) The intensity of $\hat{f}(x, y)$ is a linear function of the intensity of $g(x, y)$.

Then the solution expressed in the frequency domain is

$$\begin{aligned}\hat{F}(u, v) &= \left[\frac{H^*(u, v)S_f(u, v)}{S_f(u, v)|H(u, v)|^2 + S_\eta(u, v)} \right] G(u, v) \\ &= \left[\frac{H^*(u, v)}{|H(u, v)|^2 + S_\eta(u, v)/S_f(u, v)} \right] G(u, v)\end{aligned}$$

$H^*(u, v)$: complex conjugate of $H(u, v)$

$$|H(u, v)|^2 = H^*(u, v)H(u, v)$$

$S_\eta(u, v) = |N(u, v)|^2$ = power spectrum (or autocorrelation) of the noise

$S_f(u, v) = |F(u, v)|^2$ = power spectrum of the undegraded image

Wiener Filtering

$$\hat{F}(u, v) = \left[\frac{1}{H(u, v)} \frac{|H(u, v)|^2}{|H(u, v)|^2 + S_f(u, v) / S_\eta(u, v)} \right] G(u, v)$$

↑
undegraded
image

$S_f(u, v)$ is seldom known, although the power spectrum of white noise is constant.

When these quantities are not known or cannot be estimated, a common approach is to approximate the above equation by

$$\hat{F}(u, v) \approx \left[\frac{1}{H(u, v)} \frac{|H(u, v)|^2}{|H(u, v)|^2 + K} \right] G(u, v)$$

K is a constant that is generally specified interactively to yield the best visual results.

Note:

- The Wiener filter does not have the zero problem of inverse filter.
- If the noise is zero, the Wiener filter reduces to the inverse filter.

$$\hookrightarrow \frac{1}{H(u, v)} \frac{(H(u, v))^2}{(H(u, v))^2} = H^{-1}(u, v)$$

Derivation (1)

$$e^2 = MN \sum_x \sum_y |f(x, y) - \hat{f}(x, y)|^2$$

$$= \sum_u \sum_v |F(u, v) - \hat{F}(u, v)|^2 \quad \text{Parseval's Theorem}$$

$$= \sum_u \sum_v |F(u, v) - [F(u, v)H(u, v) + N(u, v)]W(u, v)|^2$$

$$= \sum_u \sum_v |F(u, v)[1 - H(u, v)W(u, v)] - N(u, v)W(u, v)|^2$$

$$= \sum_u \sum_v |F(u, v)[1 - H(u, v)W(u, v)]|^2 + |N(u, v)W(u, v)|^2$$

$$\frac{\partial e^2}{\partial W(u, v)} = |F|^2 [2(1 - H^*W^*)(-H)] + |N|^2 [2W^*] = 0 \quad \text{不可能} \quad \frac{\partial e^2}{\partial W(u, v)} = 0, \frac{\partial z z^*}{\partial z} = 2z^*$$

$$W^*(u, v) = \frac{|F(u, v)|^2 H(u, v)}{|F(u, v)H(u, v)|^2 + |N(u, v)|^2} \Rightarrow W(u, v) = \frac{H^*(u, v)}{|H(u, v)|^2 + \frac{|N(u, v)|^2}{|F(u, v)|^2}}$$

Derivation (2)

$$W(u, v) = \frac{1}{H(u, v)} \frac{|H(u, v)|^2}{|H(u, v)|^2 + \frac{|S_\eta(u, v)|^2}{|S_F(u, v)|^2}}$$

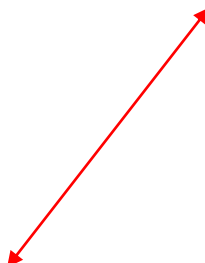
$$S_\eta = E\{N(u, v)N^*(u, v)\}$$

$$S_F = E\{F(u, v)F^*(u, v)\}$$

$$SNR = \frac{\sum_{u=0}^{M-1} \sum_{v=0}^{-1} |F(u, v)|^2}{\sum_{u=0}^{M-1} \sum_{v=0}^{-1} |N(u, v)|^2}$$

$$W(u, v) \approx \frac{1}{H(u, v)} \frac{|H(u, v)|^2}{|H(u, v)|^2 + \frac{1}{SNR}}$$

unknown



Wiener Filtering vs. Inverse Filtering



Full inverse filter

Radially limited inverse filter

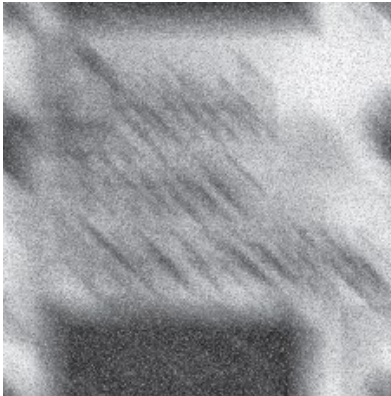
Wiener filter

a b c

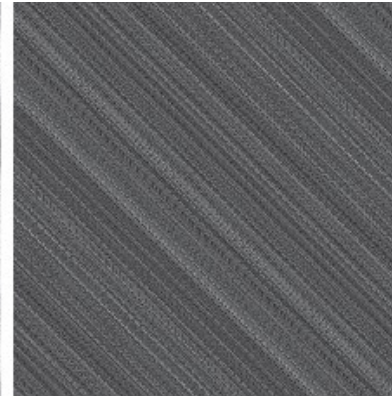
FIGURE 5.28 Comparison of inverse and Wiener filtering. (a) Result of full inverse filtering of Fig. 5.25(b). (b) Radially limited inverse filter result. (c) Wiener filter result.

Motion blur +
noise

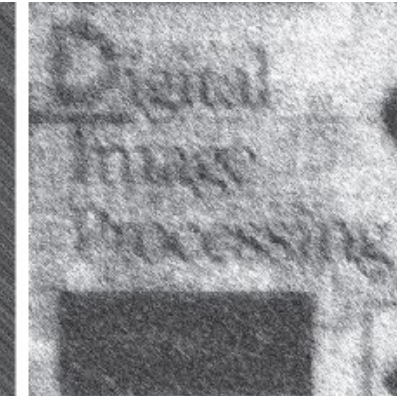
Corrupted image



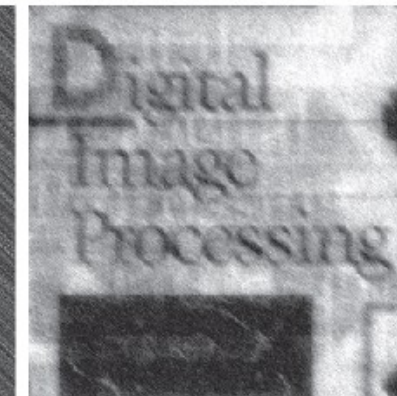
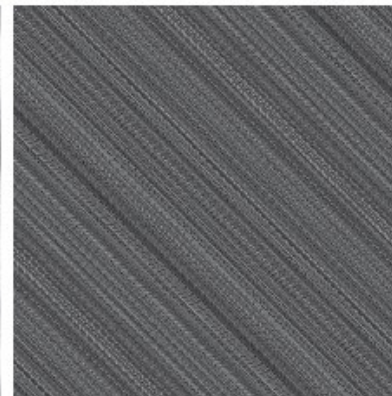
Inverse filtering



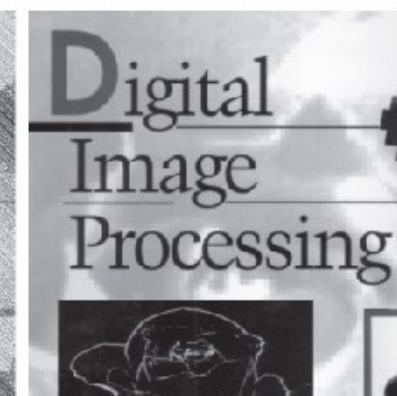
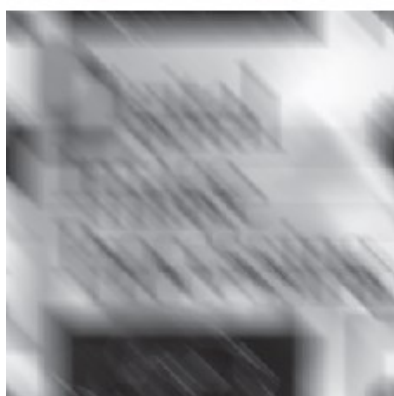
Wiener filtering



Noise variance
one order of
magnitude less



Noise variance
five order of
magnitude less



a b c
d e f
g h i

FIGURE 5.29 (a) 8-bit image corrupted by motion blur and additive noise. (b) Result of inverse filtering. (c) Result of Wiener filtering. (d)–(f) Same sequence, but with noise variance one order of magnitude less. (g)–(i) Same sequence, but noise variance reduced by five orders of magnitude from (a). Note in (h) how the deblurred image is quite visible through a “curtain” of noise.

Quality Measures

- Signal-to-Noise Ratio (SNR)

$$SNR = \frac{\sum_{u=0}^{M-1} \sum_{v=0}^{N-1} |F(u, v)|^2}{\sum_{u=0}^{M-1} \sum_{v=0}^{N-1} |N(u, v)|^2}$$

- Mean-Square Error (MSE)

$$MSE = \frac{1}{MN} \sum_{x=0}^{M-1} \sum_{y=0}^{N-1} [f(x, y) - \bar{f}(x, y)]^2$$

- Mean-Square Error (RMSE)

$$RMSE = \sqrt{\frac{1}{MN} \sum_{x=0}^{M-1} \sum_{y=0}^{N-1} [f(x, y) - \bar{f}(x, y)]^2}$$

- Root-Mean-Square-Signal-to-Noise Ratio

$$RMSSNR = \sqrt{\frac{\sum_{u=0}^{M-1} \sum_{v=0}^{N-1} f(u, v)^2}{\sum_{u=0}^{M-1} \sum_{v=0}^{N-1} |f(u, v) - \bar{f}(u, v)|^2}}$$

Constrained Least Squares Filtering (1)

- In Wiener filter, the power spectra of the undegraded image and noise must be known.
- Although a constant estimate is sometimes useful, it is not always suitable.
- Constrained least squares filtering just requires the mean and variance of the noise. It yields an optimal result to each image. (Note, however, the optimality criteria are not necessarily related to perceived image quality.)
- In the mathematical derivation, we represent an $M \times N$ image by an $MN \times 1$ column vector.

↳ 拼成一行

Constrained Least Squares Filtering (2)

In vector-matrix form,

$$\mathbf{g} = \mathbf{Hf} + \boldsymbol{\eta}$$

Formulation that aims at reducing noise sensitivity:

$$\min \sum_{x=0}^{M-1} \sum_{y=0}^{N-1} [\nabla^2 f(x, y)]^2 \text{ subject to } \|\mathbf{g} - \mathbf{H}\hat{\mathbf{f}}\|^2 = \|\boldsymbol{\eta}\|^2$$

∇^2 : Laplacian operator
to measure smoothness

Optimal solution in the frequency domain:

$$\hat{F}(u, v) = \left[\frac{H^*(u, v)}{|H(u, v)|^2 + \gamma |P(u, v)|^2} \right] G(u, v) \quad (5-89)$$

$P(u, v)$ is the Fourier transform of the function

$$p(x, y) = \begin{bmatrix} 0 & -1 & 0 \\ -1 & 4 & -1 \\ 0 & -1 & 0 \end{bmatrix}. \quad \text{Laplacian kernel}$$

- γ is a parameter to be adjusted so that the constraint is satisfied
- $P(u, v)$ and $H(u, v)$ must have the same size
- M & N must be even integers to preserve the even symmetry of $p(x, y)$.

Constrained Least Squares Filtering

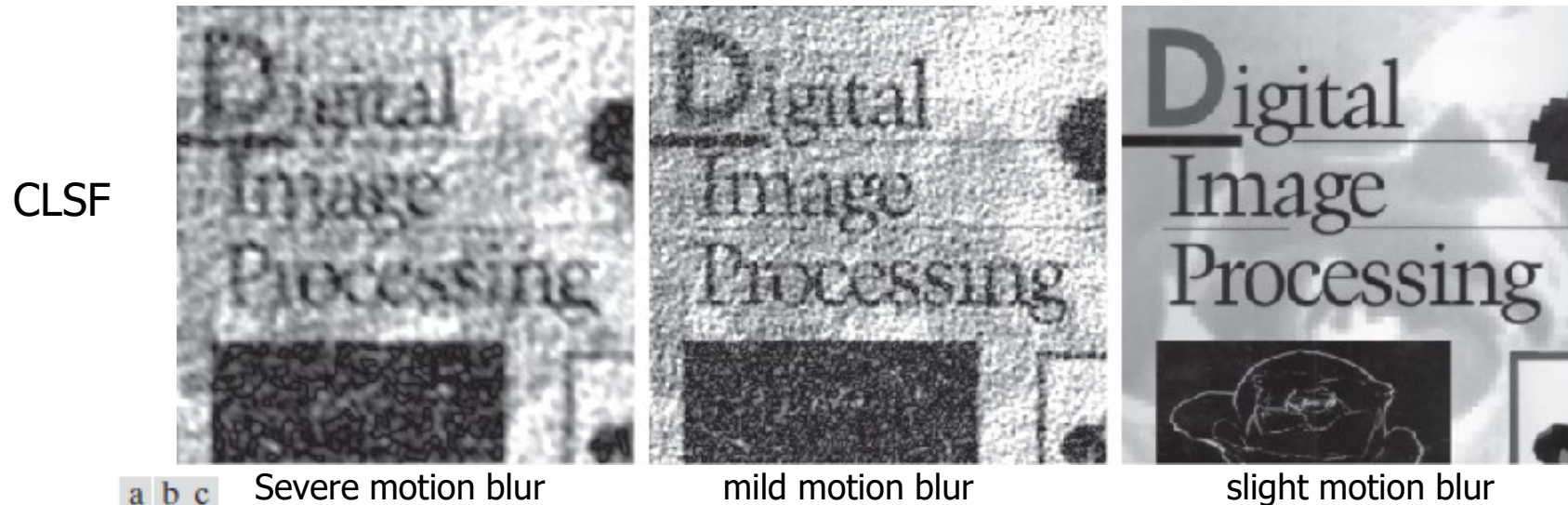
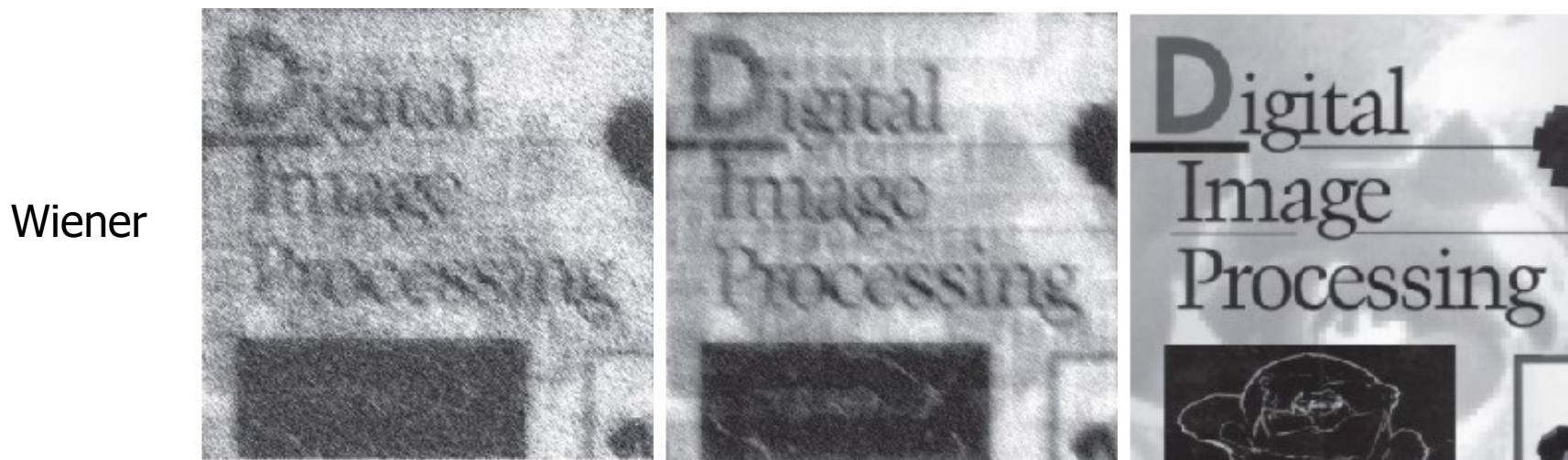


FIGURE 5.30 Results of constrained least squares filtering. Compare (a), (b), and (c) with the Wiener filtering results in Figs. 5.29(c), (f), and (i), respectively.



Computing γ Iteratively

Define a residual vector

$$\mathbf{r} \triangleq \mathbf{g} - \mathbf{H}\hat{\mathbf{f}}$$

It can be shown that

$$\phi(\gamma) \triangleq \mathbf{r}^\top \mathbf{r} = \|\mathbf{r}\|^2$$

is a monotonically increasing function. We want to adjust γ so that

$$\|\mathbf{r}\|^2 = \|\mathbf{n}\|^2 \pm \alpha \quad (5-93)$$

- tolerance

where α is an accuracy factor.

Steps:

1. Sepcify an initial value of γ .
2. Compute $\|\mathbf{r}\|^2$.
3. Stop if (5-93) is satisfied; otherwise, go to Step 4.
4. Increase γ if $\|\mathbf{r}\|^2 < (\|\mathbf{n}\|^2 - \alpha)$ or decrease γ if $\|\mathbf{r}\|^2 > (\|\mathbf{n}\|^2 + \alpha)$.
5. Go to Step 2.

Constrained Least Squares Filtering

a b

FIGURE 5.31

(a) Iteratively determined constrained least squares restoration of Fig. 5.25(b), using correct noise parameters. (b) Result obtained with wrong noise parameters.



w/ correct noise parameters

$$\sigma_{\eta}^2 = 10^{-5}$$

$$\bar{\eta} = 0$$

w/ wrong noise parameters

$$\sigma_{\eta}^2 = 10^{-2}$$

$$\bar{\eta} = 0$$

Geometric Mean Filter

- A generalization of the Wiener filter

$$F(u, v) = \left[\frac{H^*(u, v)}{|H(u, v)|^2} \right] \left[\frac{|H(u, v)|^2}{|H(u, v)|^2 + \beta [S_\eta(u, v) / S_f(u, v)]} \right]^{1-\alpha} G(u, v)$$

Geo-Mean 的概念

$\alpha = 1$: inverse filter

$\alpha = 0$: parametric Wiener filter (standard Wiener filter if $\beta = 1$)

$\alpha = 1/2$: geometric mean filter

Image Reconstruction from Projections

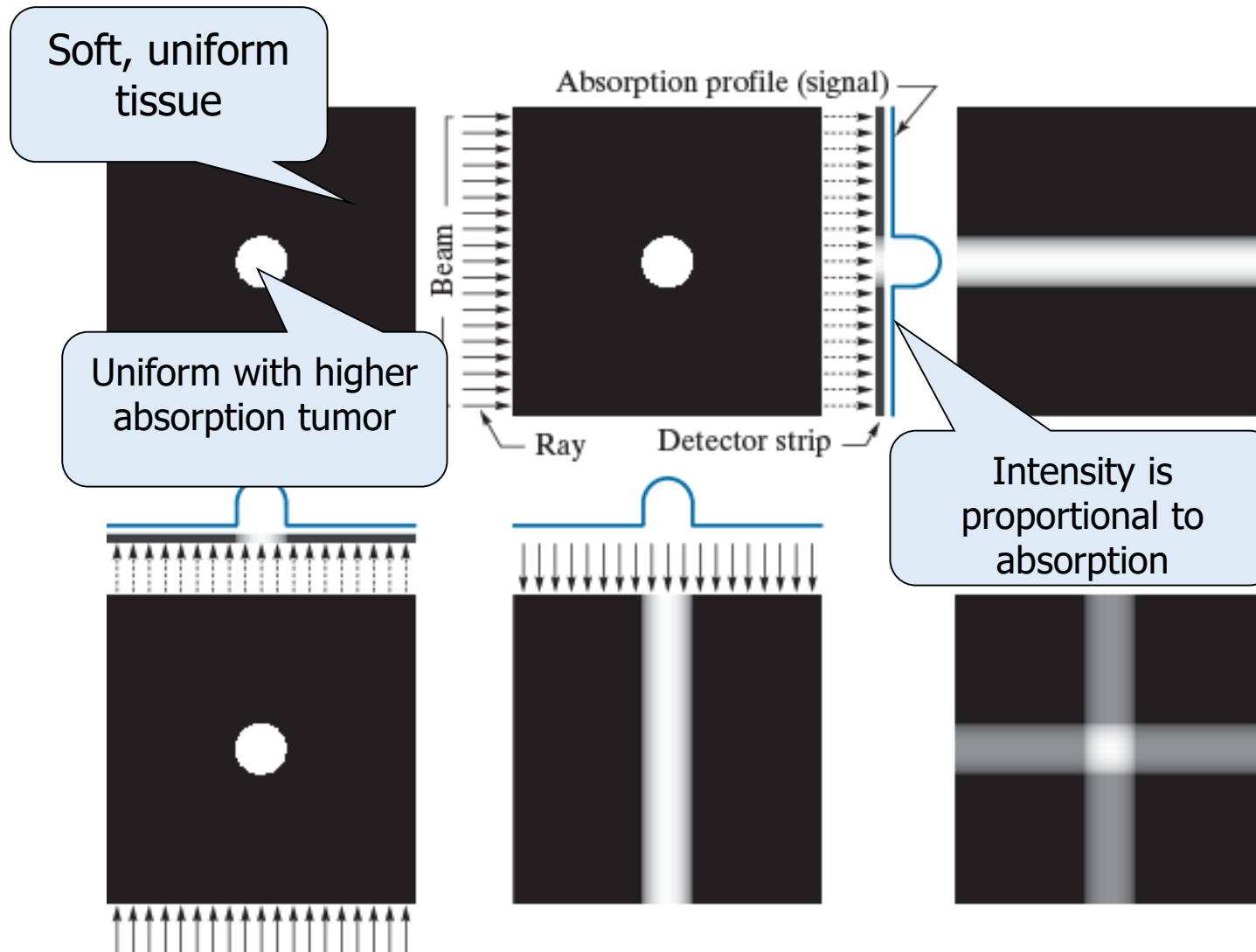
- ❑ Reconstruct an image from a series of projections by X-ray computed tomography (CT)

“Computed tomography is a medical imaging method employing tomography where digital geometry processing is used to generate a three-dimensional image of the internals of an object from a large series of two-dimensional X-ray images taken around a single axis of rotation.” --Wikipedia

- ❑ Backprojection

“ In computed tomography or other imaging techniques requiring reconstruction from multiple projections, an algorithm for calculating the contribution of each voxel of the structure to the measured ray data, to generate an image; the oldest and simplest method of image reconstruction.” --medilexicon

Image Reconstruction from Projections



a b c
d e f

FIGURE 5.32

- (a) Flat region with a single object.
- (b) Parallel beam, detector strip, and profile of sensed 1-D absorption signal.
- (c) Result of back-projecting the absorption profile.
- (d) Beam and detectors rotated by 90°.
- (e) Backprojection.
- (f) The sum of (c) and (e), intensity-scaled. The intensity where the backprojections intersect is twice the intensity of the individual back-projections.

Image Reconstruction from Projections

a b c
d e f

FIGURE 5.33

- (a) Same as Fig. 5.32(a).
(b)-(e) Reconstruction using 1, 2, 3, and 4 back-projections 45° apart.
(f) Reconstruction with 32 backprojections 5.625° apart (note the blurring).

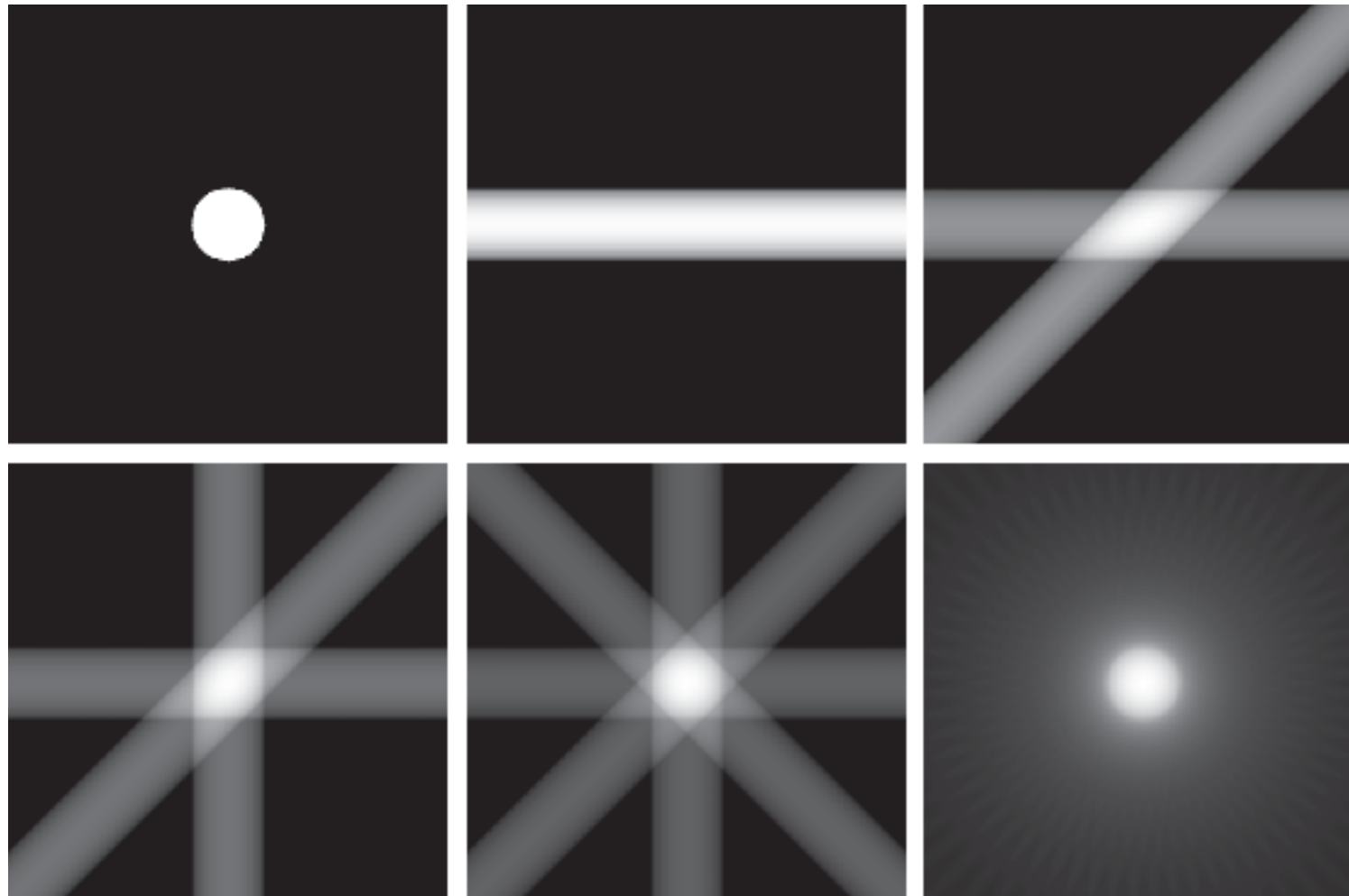
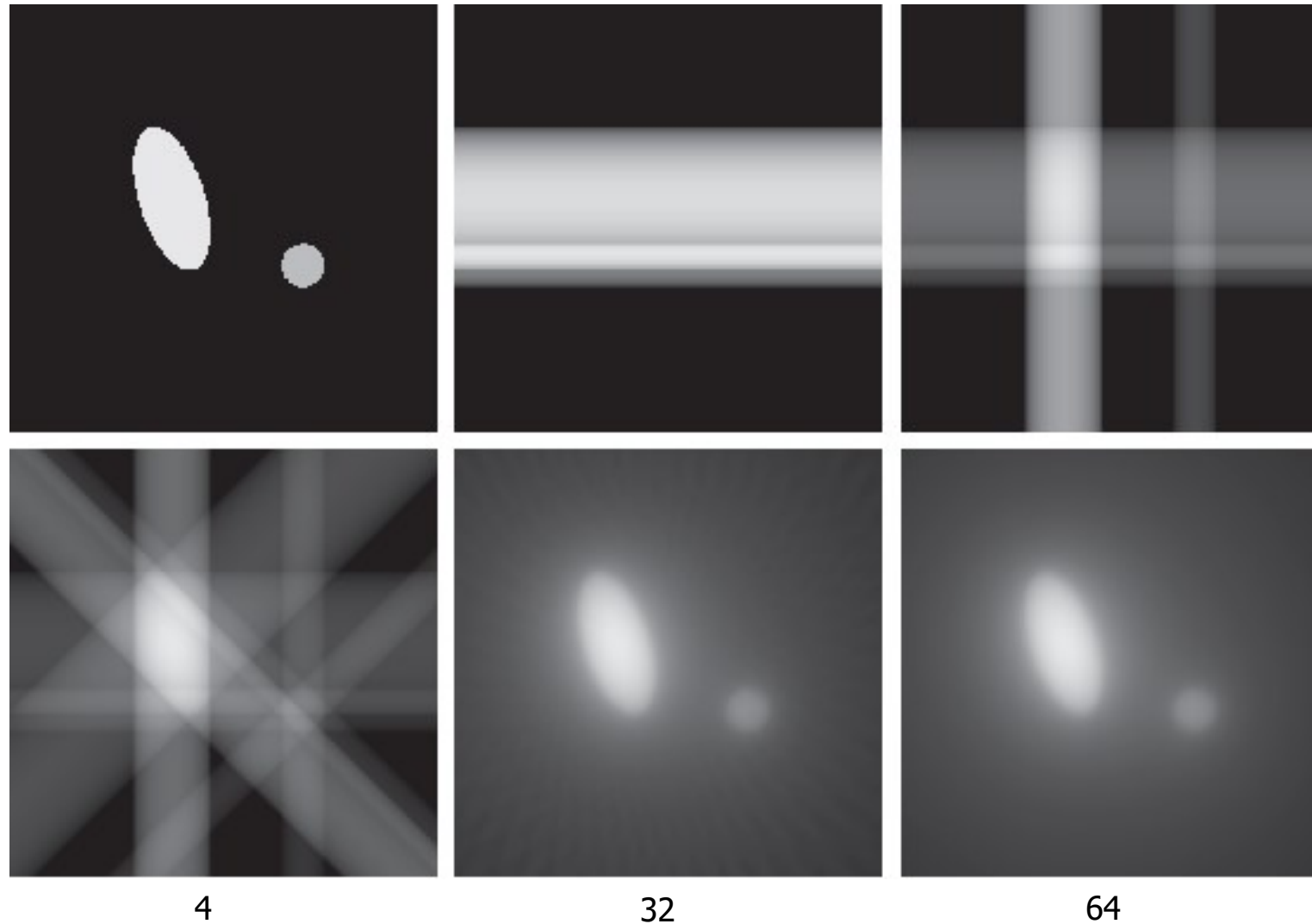


Image Reconstruction from Projections

a	b	c
d	e	f

FIGURE 5.34

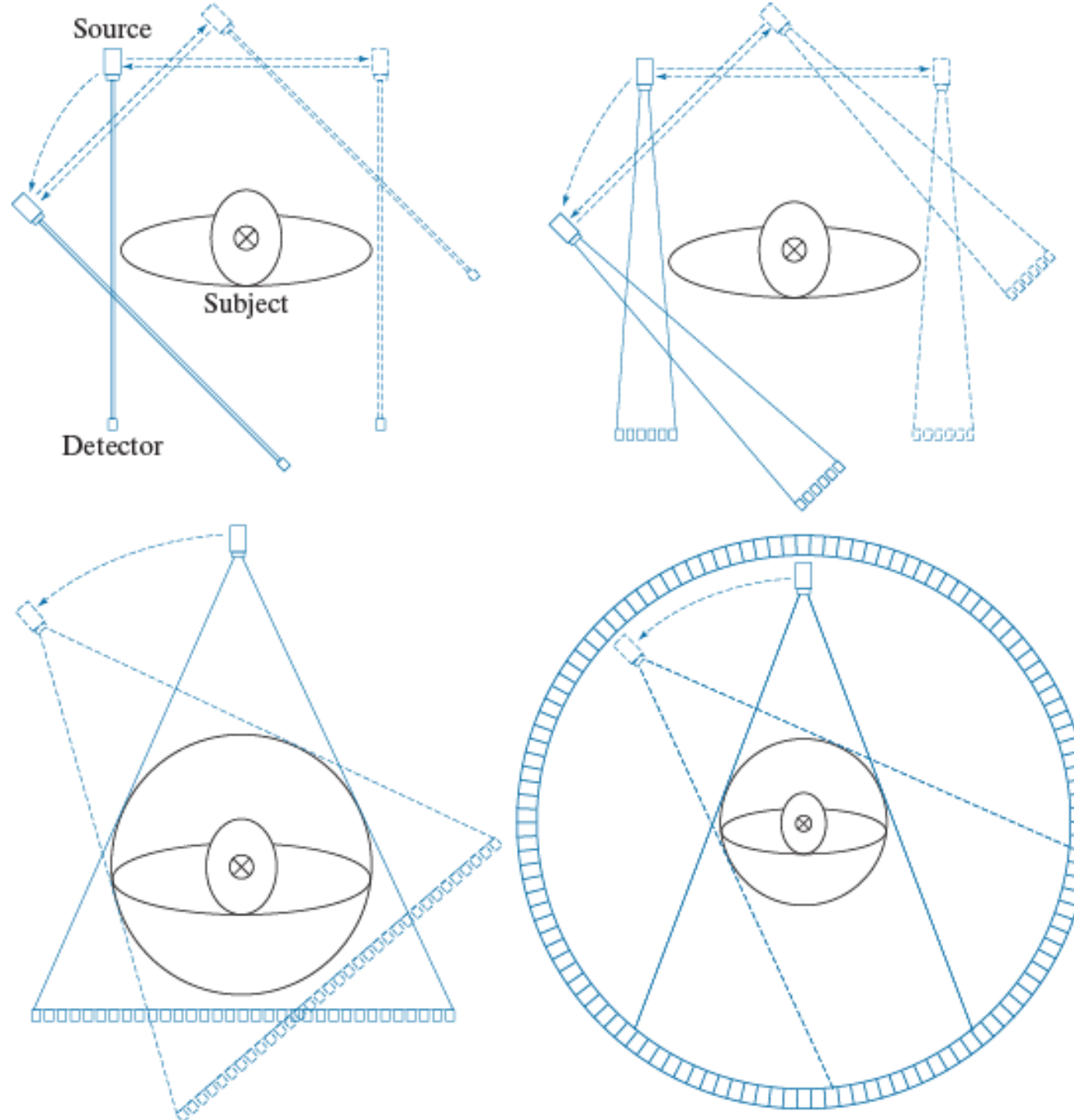
- (a) Two objects with different absorption characteristics.
(b)–(d) Reconstruction using 1, 2, and 4 backprojections, 45° apart.
(e) Reconstruction with 32 backprojections, 5.625° apart.
(f) Reconstruction with 64 backprojections, 2.8125° apart.



a
b
c
d

FIGURE 5.35

Four generations of CT scanners. The dotted arrow lines indicate incremental linear motion. The dotted arrow arcs indicate incremental rotation. The cross-mark on the subject's head indicates linear motion perpendicular to the plane of the paper. The double arrows in (a) and (b) indicate that the source/detector unit is translated and then brought back into its original position.



Other CTs

- ❑ **Electron beam CT** (fifth-generation CT)

Electron beam tomography (EBCT) was introduced in the early 1980s, by medical physicist Andrew Castagnini, as a method of improving the **temporal resolution** of CT scanners. High cost and poor flexibility.

- ❑ **Helical (or spiral) cone beam computed tomography** (sixth-generation)

A type of three dimensional computed tomography (CT) in which the source (usually of x-rays) describes a helical trajectory relative to the object while a two dimensional array of detectors measures the transmitted radiation on part of a cone of rays emitting from the source – Wikipedia

- ❑ **Multislice CT** (seventh-generation)

major strengths:

- Significant increase in detail
- Utilizes X-ray tubes more economically
- Reducing cost and potentially reducing dosage

Projections and the Radon Transform (1)

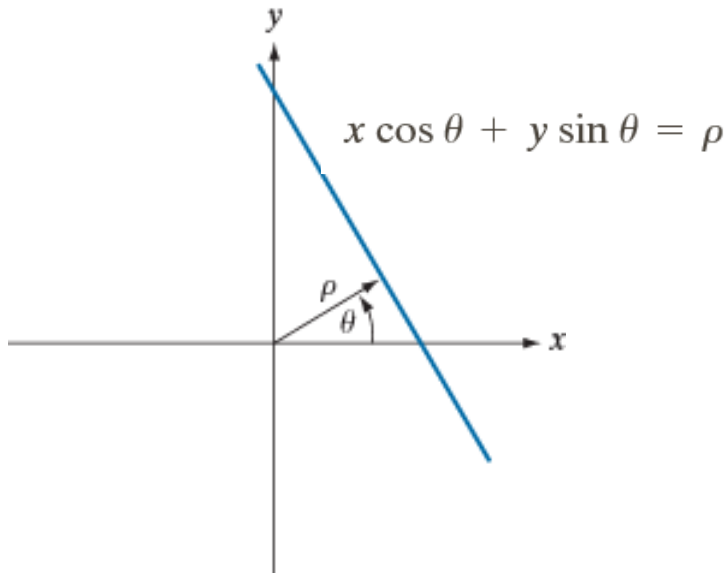
- Mathematics behind CT
- The basic principle of single photon emission tomography (SPECT), positron emission tomography (PET), magnetic resonance imaging (MRI), and some ultrasound imaging.
- In mathematics, the **Radon transform** is the [integral transform](#) which takes a function f defined on the plane to a function $R\{f\}$ defined on the (two-dimensional) space of lines in the plane, whose value at a particular line is equal to the [line integral](#) of the function over that line. The transform was introduced in 1917 by Johann Radon. -- Wikipedia



Projections and the Radon Transform (2)

FIGURE 5.36

Normal representation of a line.



Complete projection, $g(\rho, \theta_k)$, for a fixed angle

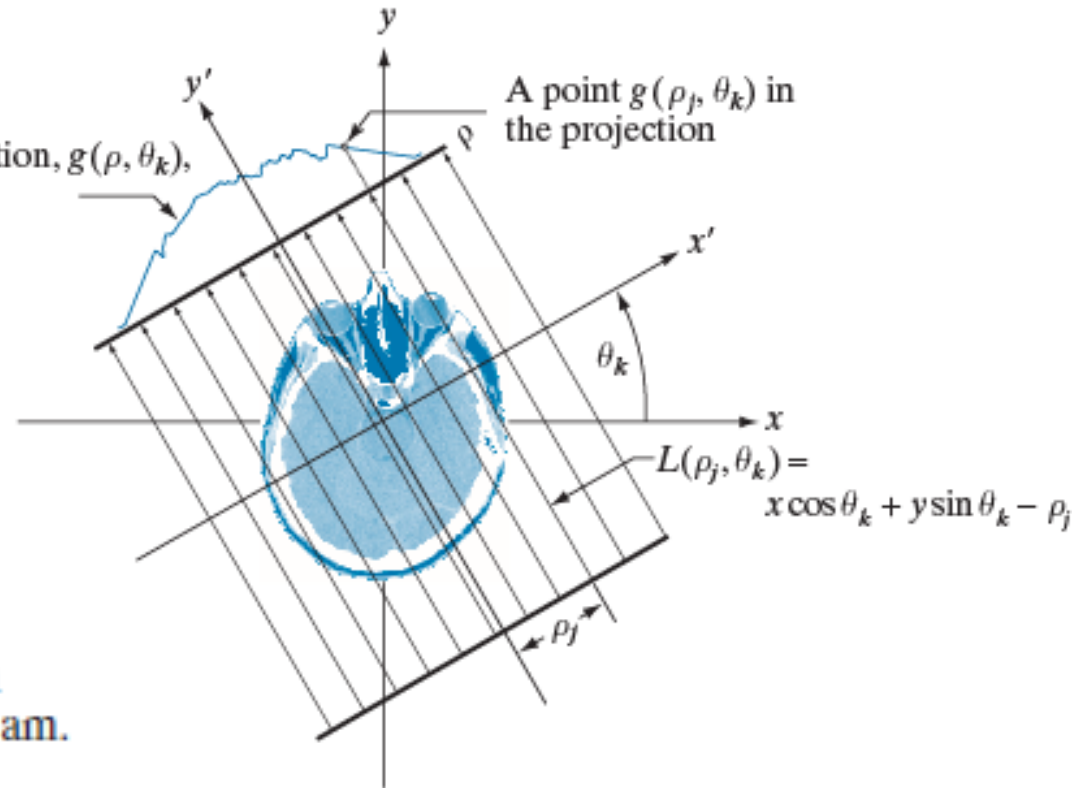


FIGURE 5.37
Geometry of a parallel-ray beam.

A point (ρ_j, θ_k) on the projection curve is the raysum (a line integral) along the line:

$$g(\rho_j, \theta_k) = \int_{-\infty}^{\infty} \int_{-\infty}^{\infty} f(x, y) \delta(x \cos \theta_k + y \sin \theta_k - \rho_j) dx dy$$

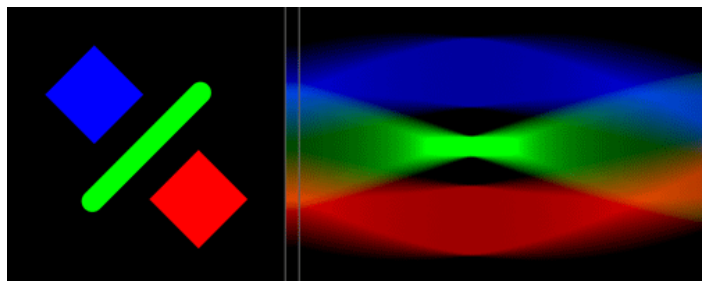
$f(x, y)$:沿着這方向 project 出來的值 = g

Projections and the Radon Transform (3)

- **Radon transform** gives the projection (line integral) of $f(x,y)$ along an arbitrary line in the xy -plane

$$\mathcal{R}\{f\} = g(\rho, \theta) = \int_{-\infty}^{\infty} \int_{-\infty}^{\infty} f(x, y) \delta(x \cos \theta + y \sin \theta - \rho) dx dy$$

$$\mathcal{R}\{f\} = g(\rho, \theta) = \sum_{x=0}^{M-1} \sum_{y=0}^{N-1} f(x, y) \delta(x \cos \theta + y \sin \theta - \rho) \quad (5-103)$$



Horizontal projections through the shape result in an accumulated signal (middle bar). The **sinogram** on the right is generated by collecting many such projections as the shape rotates. Here, color is used to highlight which object is producing which part of the signal. Note how straight features, when aligned with the projection direction, result in stronger signals.

Example: Using the Radon transform to obtain the projection of a circular region

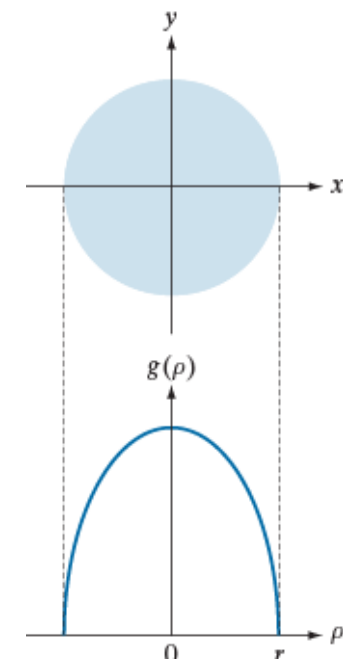
- Assume that the circle is centered on the origin of the xy-plane. Because the object is circularly symmetric, its projections are the same for all angles, so we just check the projection for $\theta = 0^\circ$.

$$f(x, y) = \begin{cases} A & x^2 + y^2 \leq r^2 \\ 0 & \text{otherwise} \end{cases}$$

$$\begin{aligned} g(\rho, \theta) &= \int_{-\infty}^{\infty} \int_{-\infty}^{\infty} f(x, y) \delta(x \cos \theta + y \sin \theta - \rho) dx dy \\ &= \int_{-\infty}^{\infty} \int_{-\infty}^{\infty} f(x, y) \delta(x - \rho) dx dy \\ &= \int_{-\infty}^{\infty} f(\rho, y) dy = \int_{-\sqrt{r^2 - \rho^2}}^{\sqrt{r^2 - \rho^2}} f(\rho, y) dy = \int_{-\sqrt{r^2 - \rho^2}}^{\sqrt{r^2 - \rho^2}} Ady \\ &= \begin{cases} 2A\sqrt{r^2 - \rho^2} & |\rho| \leq r \\ 0 & \text{otherwise} \end{cases} \end{aligned}$$

a
b

FIGURE 5.38
 (a) A disk and,
 (b) a plot of its Radon transform, derived
 analytically. Here we
 were able to plot the
 transform because it
 depends only on one
 variable. When g
 depends on both ρ and
 θ , the Radon transform
 becomes an image
 whose axes are ρ and
 θ , and the intensity of
 a pixel is proportional
 to the value of g at the
 location of that pixel.



Sinogram: The Result of Radon Transform

- **Sinogram:** the result of displaying Radon transform as an image with ρ and θ as rectilinear coordinates

a	b
c	d

FIGURE 5.39
 Two images and their sinograms (Radon transforms). Each row of a sinogram is a projection along the corresponding angle on the vertical axis. (Note that the horizontal axis of the sinograms are values of ρ .) Image (c) is called the *Shepp-Logan phantom*. In its original form, the contrast of the phantom is quite low. It is shown enhanced here to facilitate viewing.

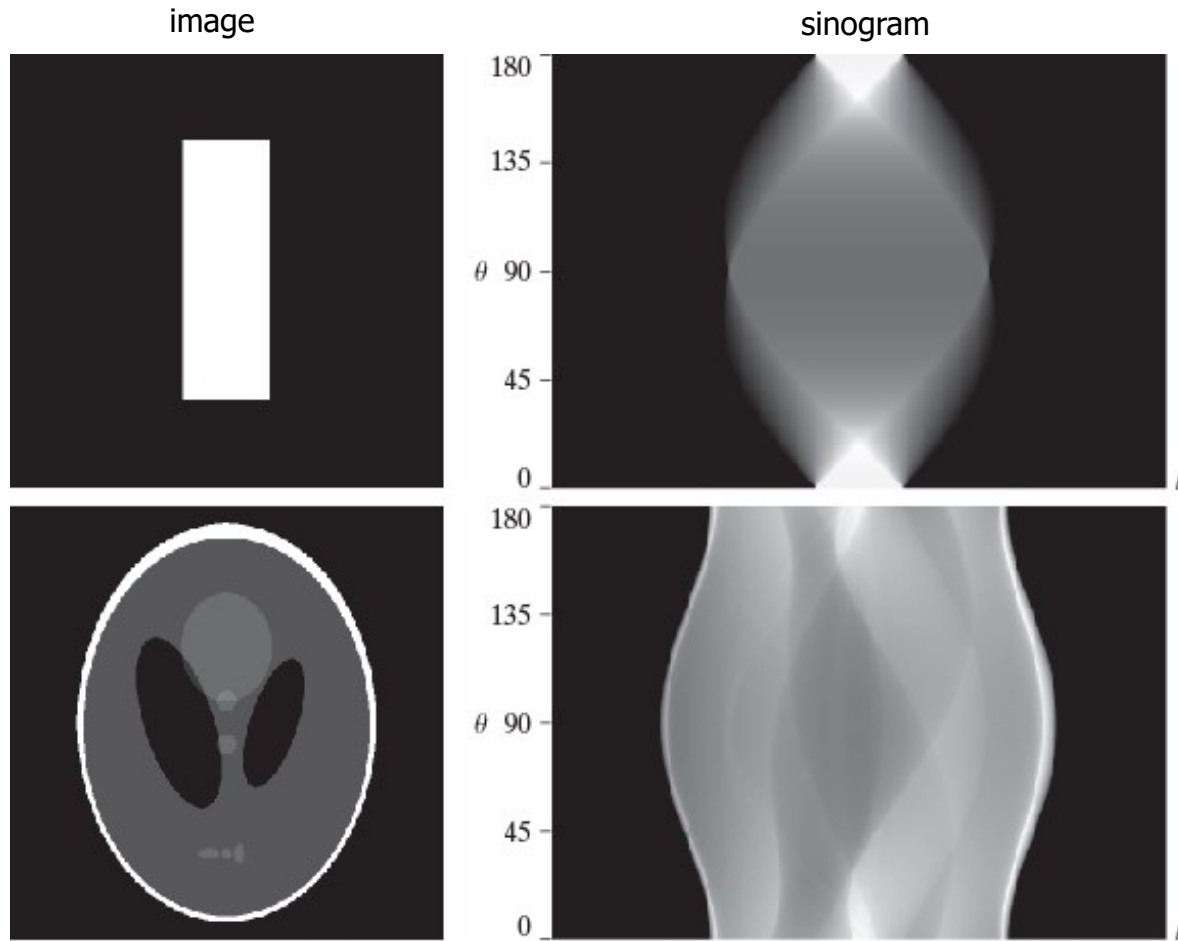


Image Reconstruction (Backprojection)

Obtain a formal expression of a backprojected image from the Radon transform. Consider a single point $g(\rho_j, \theta_k)$. Backprojecting this point is to copy $L(\rho_j, \theta_k)$ onto the image, where the value of each point on the line is $g(\rho_j, \theta_k)$. Repeating the process for all ρ_j 's for a fixed θ_k yields

$$f_{\theta_k}(x, y) = g(\rho, \theta_k) = g(x \cos \theta_k + y \sin \theta_k, \theta_k)$$

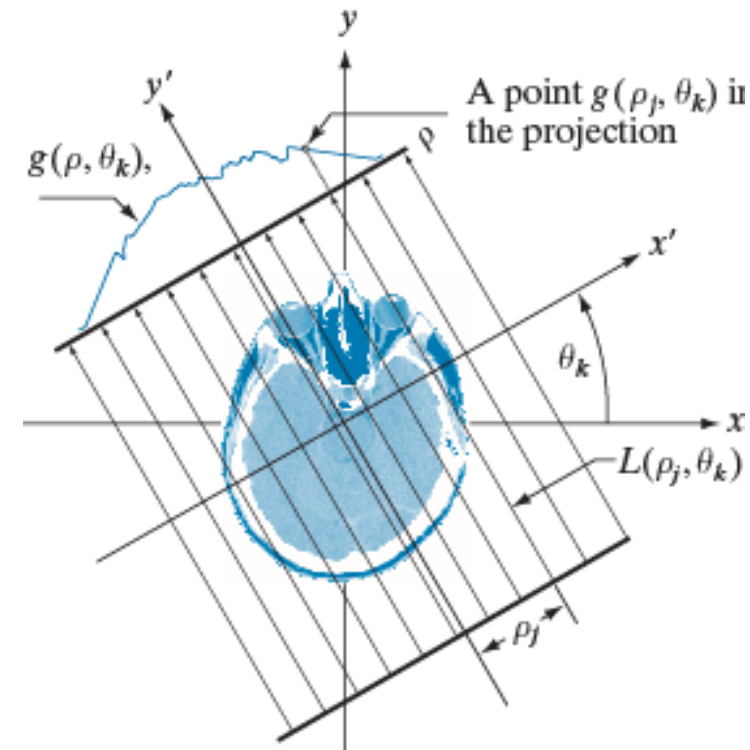
The equation holds for any value of θ_k :

$$f_\theta(x, y) = g(x \cos \theta + y \sin \theta, \theta)$$

Integrating over all angles:

$$f(x, y) = \int_0^\pi f_\theta(x, y) d\theta$$

$$f(x, y) = \sum_{\theta=0}^{\pi} f_\theta(x, y) \quad (5-106)$$

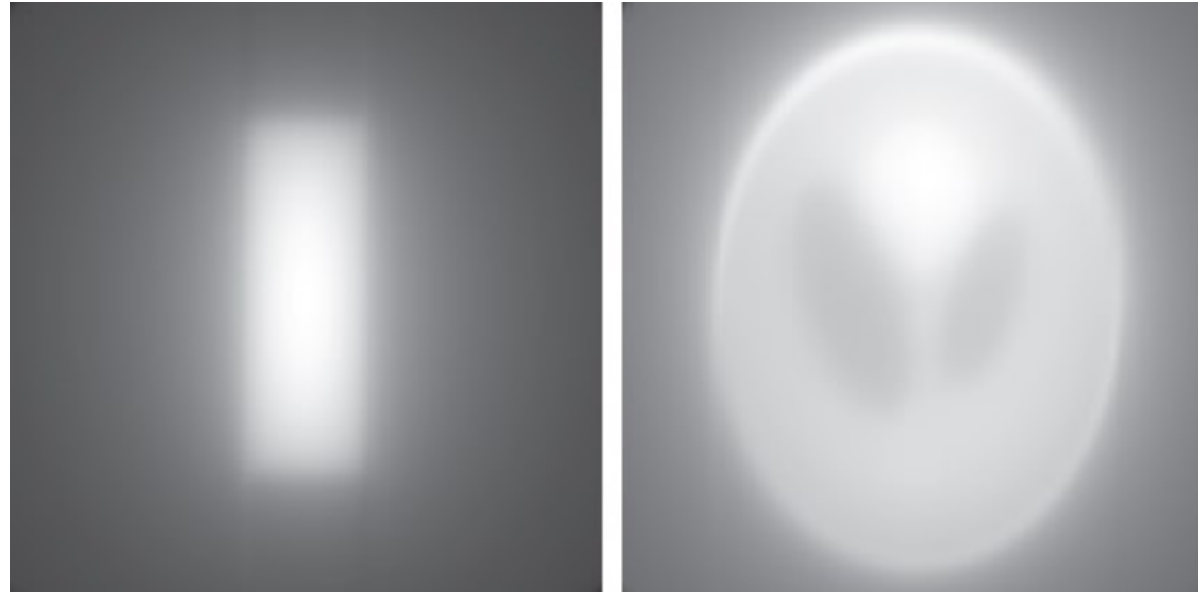


A back-projected image formed is referred to as a **laminogram**, which is only an approximation of the original image.

Example Laminograms

a b

FIGURE 5.40
Backprojections
of the sinograms
in Fig. 5.39.



⇒ A straightforward use of Eqs. (5-103) and (5-106) does not yield acceptable results.

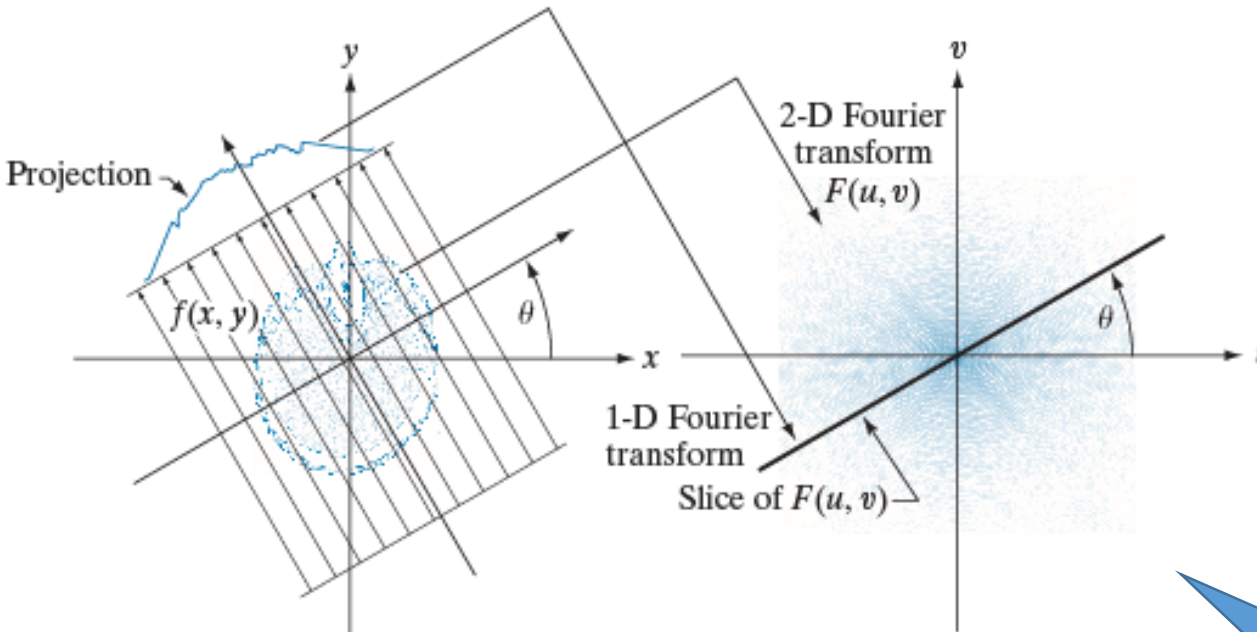
The Fourier-Slice Theorem

For a given value of θ , the 1-D Fourier transform of a projection with respect to ρ is

$$\begin{aligned} G(\omega, \theta) &= \int_{-\infty}^{\infty} g(\rho, \theta) e^{-j2\pi\omega\rho} d\rho \\ &= \int_{-\infty}^{\infty} \int_{-\infty}^{\infty} \int_{-\infty}^{\infty} f(x, y) \delta(x \cos \theta + y \sin \theta - \rho) e^{-j2\pi\omega\rho} d\rho dx dy \\ &= \int_{-\infty}^{\infty} \int_{-\infty}^{\infty} f(x, y) \left[\int_{-\infty}^{\infty} \delta(x \cos \theta + y \sin \theta - \rho) e^{-j2\pi\omega\rho} d\rho \right] dx dy \\ &= \int_{-\infty}^{\infty} \int_{-\infty}^{\infty} f(x, y) e^{-j2\pi\omega(x \cos \theta + y \sin \theta)} dx dy \\ &= \left[\int_{-\infty}^{\infty} \int_{-\infty}^{\infty} f(x, y) e^{-j2\pi(ux+vy)} dx dy \right]_{u=\omega \cos \theta, v=\omega \sin \theta} \\ &= [F(u, v)]_{u=\omega \cos \theta, v=\omega \sin \theta} \\ &= F(\omega \cos \theta, \omega \sin \theta) \end{aligned}$$

The Fourier-Slice Theorem

FIGURE 5.41
Illustration of the Fourier-slice theorem. The 1-D Fourier transform of a projection is a slice of the 2-D Fourier transform of the region from which the projection was obtained. Note the correspondence of the angle θ in the two figures.



The basis of reconstruction

Fourier-slice theorem: The Fourier transform of a projection is a slice of the 2-D Fourier transform of the region from which the projection was obtained

$$G(\omega, \theta) = [F(u, v)]_{u=\omega \cos \theta, v=\omega \sin \theta} = F(\omega \cos \theta, \omega \sin \theta)$$

Reconstruction Using Parallel-Beam Filtered Backprojections

More efficient than taking the inverse Fourier transform of $F(u,v)$.

$$f(x,y) = \int_{-\infty}^{\infty} \int_{-\infty}^{\infty} F(u,v) e^{j2\pi(ux+vy)} du dv$$

代入
u = ωcosθ, v = ωsinθ ⇒ du dv = ωdωdθ

$$f(x,y) = \int_0^{2\pi} \int_0^{\infty} F(\omega \cos \theta, \omega \sin \theta) e^{j2\pi\omega(x \cos \theta + y \sin \theta)} \omega d\omega d\theta$$

$$= \int_0^{2\pi} \int_0^{\infty} G(\omega, \theta) e^{j2\pi\omega(x \cos \theta + y \sin \theta)} \omega d\omega d\theta$$

$$\because G(\omega, \theta + 180^\circ) = G(-\omega, \theta)$$

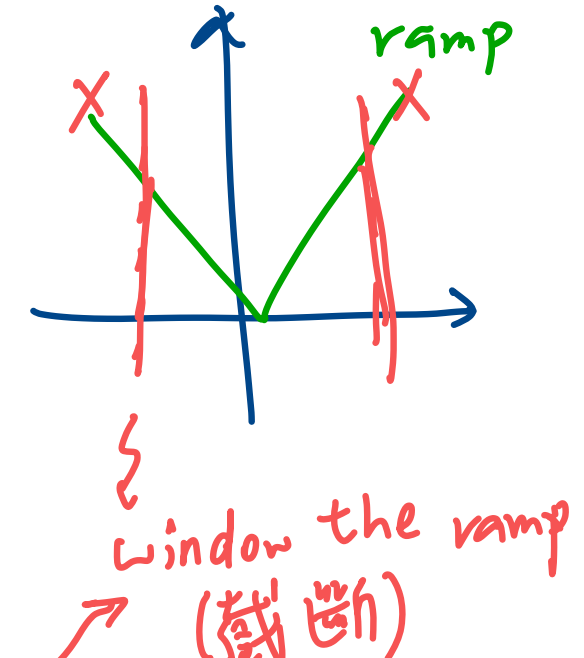
∴ 对称

$$f(x,y) = \int_0^{\pi} \int_{-\infty}^{\infty} |\omega| G(\omega, \theta) e^{j2\pi\omega(x \cos \theta + y \sin \theta)} d\omega d\theta$$

$$= \int_0^{\pi} \left[\int_{-\infty}^{\infty} |\omega| G(w, \theta) e^{j2\pi w \rho} dw \right]_{\rho=x \cos \theta + y \sin \theta} d\theta$$

!|ω|
It's not integrable

Approach: Window the ramp so it becomes zero outside of a defined frequency interval. The window band-limits the ramp filter.



Hamming / Hann Window

$$h(\omega) = \begin{cases} c + (c-1) \cos \frac{2\pi\omega}{M-1} & 0 \leq \omega \leq (M-1) \\ 0 & \text{otherwise} \end{cases}$$

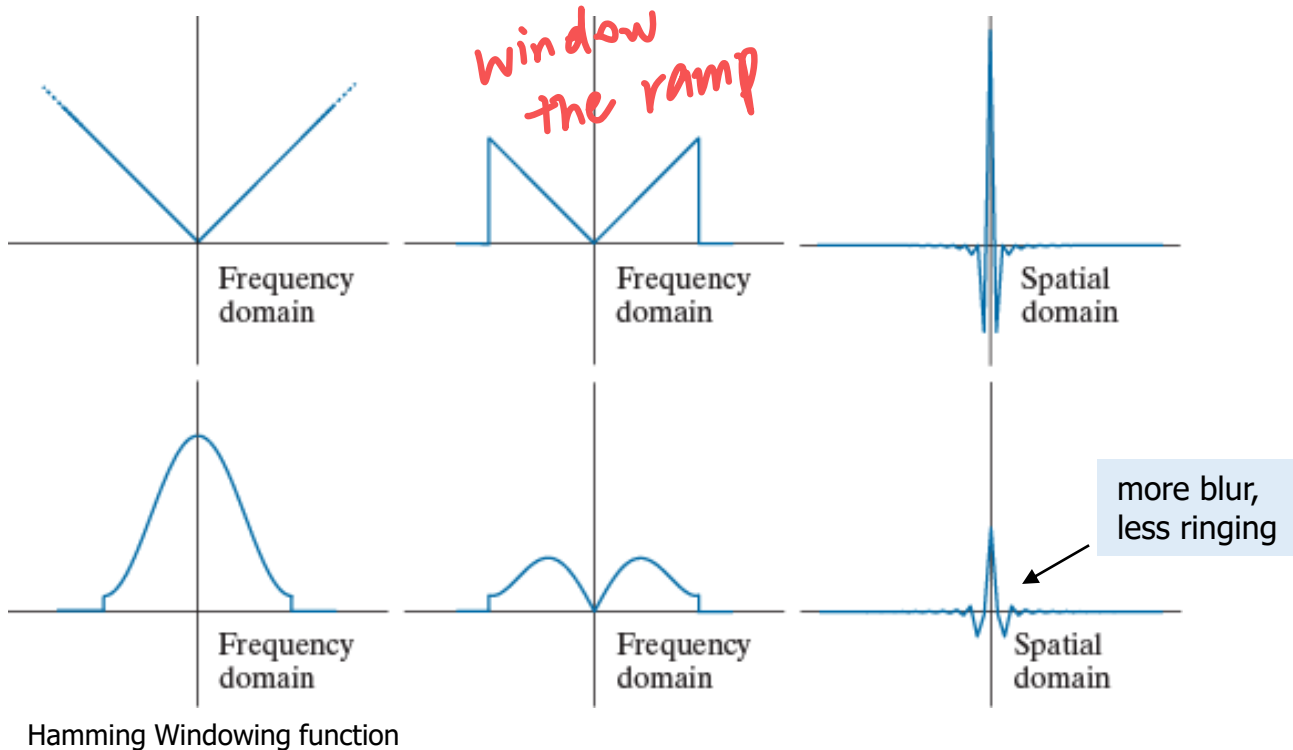
$c = 0.54 \Rightarrow$ Hamming window

$c = 0.5 \Rightarrow$ Hann window

a b c
d e f

FIGURE 5.42

- (a) Frequency domain ramp filter transfer function.
(b) Function after band-limiting it with a box filter.
(c) Spatial domain representation.
(d) Hamming windowing function.
(e) Windowed ramp filter, formed as the product of (b) and (d).
(f) Spatial representation of the product. (Note the decrease in ringing.)



Filtered Backprojection

The complete, filtered backprojection (to obtain the reconstructed image $f(x,y)$) consists of the following steps:

1. Compute the 1-D Fourier transform of each projection
2. Multiply each Fourier transform by the filter function $|\omega|$ multiplied by a suitable (e.g., Hamming) window
3. Obtain the inverse 1-D Fourier transform of each resulting filtered transform
4. Integrate (sum) all the 1-D inverse transforms from Step 3

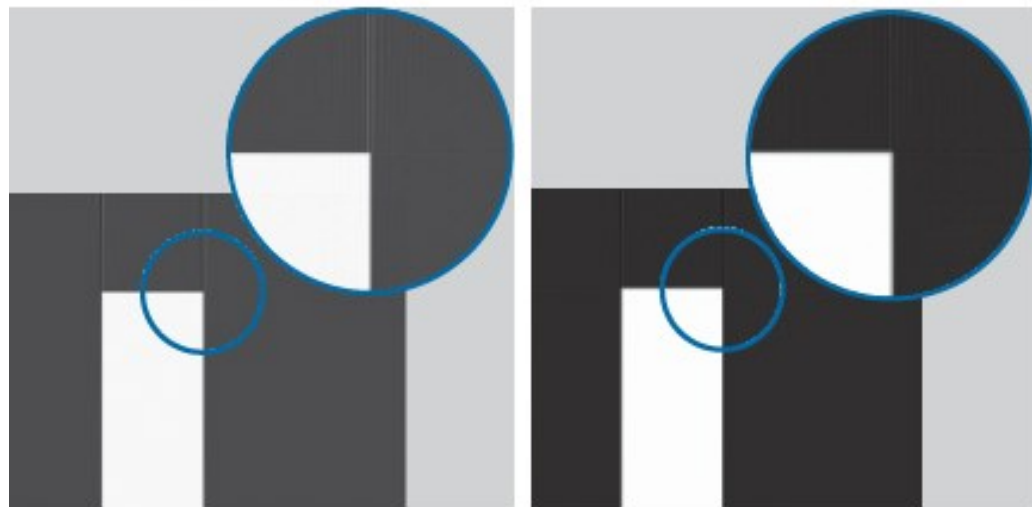
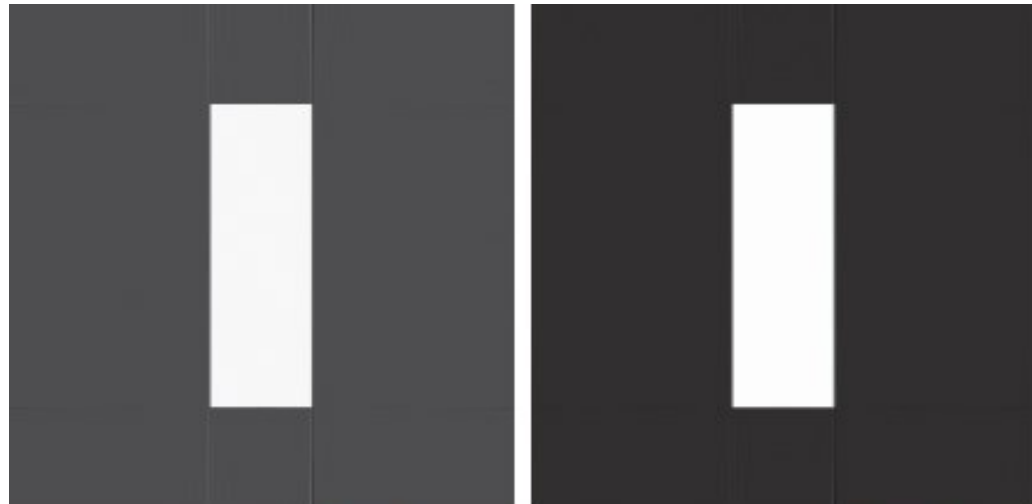
Examples: Filtered Backprojection

a b
c d

FIGURE 5.43
Filtered backprojections of the rectangle using (a) a ramp filter, and (b) a Hamming windowed ramp filter. The second row shows zoomed details of the images in the first row. Compare with Fig. 5.40(a).



Fig. 5.40(a)



Band-limited ramp filter

Hamming windowed ramp filter

Examples: Filtered Backprojection

a b

FIGURE 5.44
Filtered backprojections of the head phantom using (a) a ramp filter, and (b) a Hamming windowed ramp filter. Compare with Fig. 5.40(b)



Band-limited ramp filter Hamming windowed ramp filter

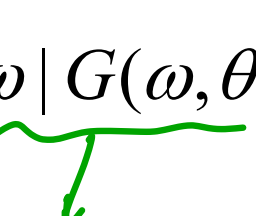


Fig. 5.40(b)

Direct backprojection

Implementation of Filtered Backprojection in Spatial Domain

- Fourier transform of the product of two frequency domain functions is equal to the convolution of the spatial representation
- Let $s(\rho)$ denote the inverse Fourier transform of $|\omega|$

$$\begin{aligned} f(x, y) &= \int_0^\pi \left[\int_{-\infty}^{\infty} |\omega| G(\omega, \theta) e^{j2\pi\omega\rho} d\omega \right]_{\rho=x\cos\theta+y\sin\theta} d\theta \\ &= \int_0^\pi [s(\rho) \star g(\rho, \theta)]_{\rho=x\cos\theta+y\sin\theta} d\theta \\ &= \int_0^\pi \left[\int_{-\infty}^{\infty} g(\rho, \theta) s(x\cos\theta + y\sin\theta - \rho) d\rho \right] d\theta \end{aligned}$$


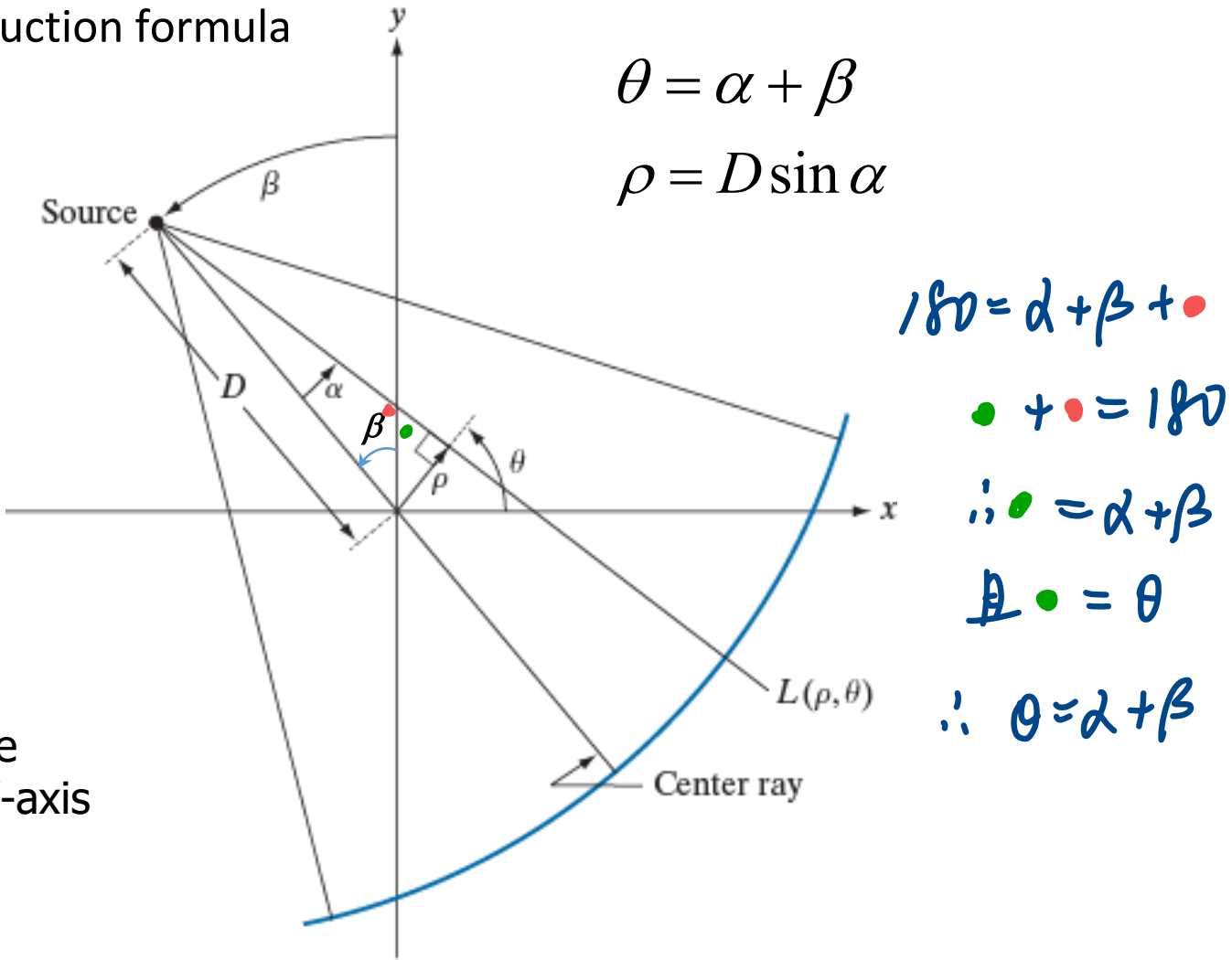
Reconstruction Using Fan-Beam Filtered Backprojections (1)

- Modern CT uses fan-beam, not parallel beam
- The detectors span a full circle
- Need to derive a new reconstruction formula

FIGURE 5.45

Basic fan-beam geometry. The line passing through the center of the source and the origin (assumed here to be the center of rotation of the source) is called the *center ray*.

β : orientation of the source wrt the Y-axis



Reconstruction Using Fan-Beam Filtered Backprojections (2)

W.L.O.G., suppose objects are encompassed within a circular area of radius T about the origin of the plane, or $g(\rho, \theta) = 0$ for $|\rho| > T$

$$\begin{aligned} f(x, y) &= \int_0^\pi \left[\int_{-\infty}^{\infty} g(\rho, \theta) s(x \cos \theta + y \sin \theta - \rho) d\rho \right] d\theta \\ &= \frac{1}{2} \underbrace{\int_0^{2\pi} \int_{-T}^T g(\rho, \theta) s(x \cos \theta + y \sin \theta - \rho) d\rho d\theta}_{\text{Let } x = r \cos \varphi \text{ and } y = r \sin \varphi} \end{aligned}$$

Let $x = r \cos \varphi$ and $y = r \sin \varphi$

$$\begin{aligned} x \cos \theta + y \sin \theta &= r \cos \varphi \cos \theta + r \sin \varphi \sin \theta \\ &= r \cos(\varphi - \theta) \end{aligned}$$

$$f(x, y) = \frac{1}{2} \int_0^{2\pi} \int_{-T}^T g(\rho, \theta) s[r \cos(\varphi - \theta) - \rho] d\rho d\theta$$

Reconstruction Using Fan-Beam Filtered Backprojections (3)

FIGURE 5.46
Maximum value
of α needed to
encompass a
region of interest.

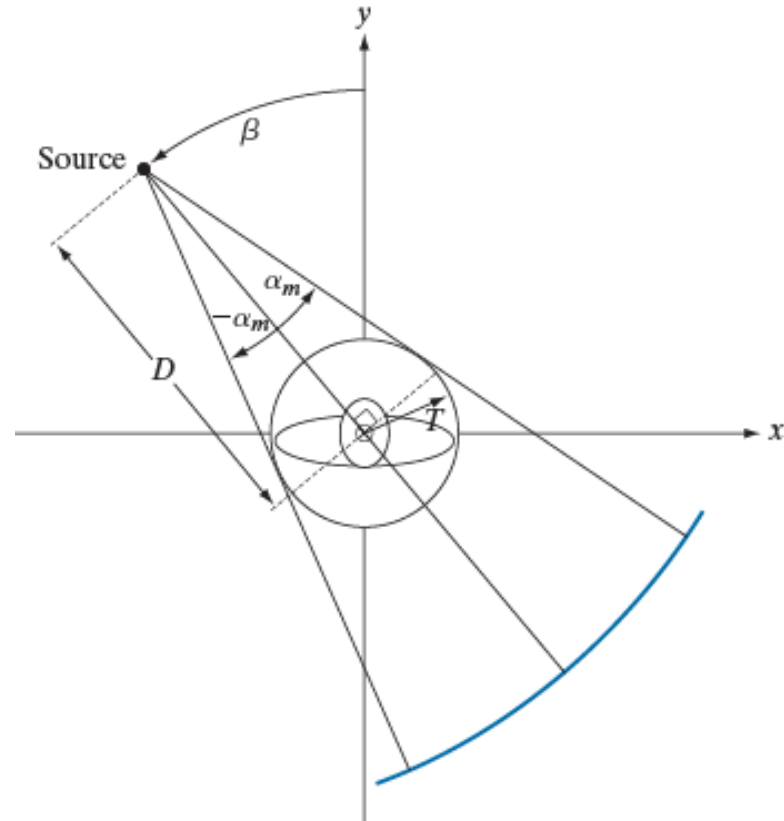
$$x = r \cos \varphi, y = r \sin \varphi$$

$$\theta = \alpha + \beta, \rho = D \sin \alpha \Rightarrow d\rho d\theta = D \cos \alpha d\alpha d\beta$$

$$f(x, y) = \frac{1}{2} \int_0^{2\pi} \int_{-T}^T g(\rho, \theta) s[r \cos(\varphi - \theta) - \rho] d\rho d\theta$$

$$f(r, \phi) = \frac{1}{2} \int_{-\alpha}^{2\pi - \alpha} \int_{-\sin^{-1}(-T/D)}^{\sin^{-1}(T/D)} g(D \sin \alpha, \alpha + \beta) s[r \cos(\alpha + \beta - \phi) - D \sin \alpha] D \cos \alpha d\alpha d\beta$$

$$f(r, \phi) = \frac{1}{2} \int_0^{2\pi} \int_{-\alpha_m}^{\alpha_m} g(D \sin \alpha, \alpha + \beta) s[r \cos(\alpha + \beta - \phi) - D \sin \alpha] D \cos \alpha d\alpha d\beta$$



Reconstruction Using Fan-Beam Filtered Backprojections (4)

Let $p(\alpha, \beta)$ denote a fan-beam projection. Because a raysum is the sum of all values along a line, it follows that regardless of the coordinate system in which it is expressed, $p(\alpha, \beta) = g(\rho, \theta)$. Thus

$$f(r, \varphi) = \frac{1}{2} \int_0^{2\pi} \int_{-\alpha_m}^{\alpha_m} p(\alpha, \beta) s(r \cos(\alpha + \beta - \varphi) - D \sin \alpha) D \cos \alpha d\alpha d\beta$$

From Fig. 5.47,

$$f(r, \varphi) = \frac{1}{2} \int_0^{2\pi} \int_{-\alpha_m}^{\alpha_m} p(\alpha, \beta) s(R \sin(\alpha' - \alpha)) D \cos \alpha d\alpha d\beta$$

$$s(R \sin \alpha) = \left(\frac{\alpha}{R \sin \alpha} \right)^2 s(\alpha)$$

$$h(\alpha) \triangleq \frac{1}{2} \left(\frac{\alpha}{\sin \alpha} \right)^2 s(\alpha)$$

$$q(\alpha, \beta) \triangleq p(\alpha, \beta) D \cos \alpha$$

$$f(r, \varphi) = \int_0^{2\pi} \frac{1}{R^2} \left[\int_{-\alpha_m}^{\alpha_m} q(\alpha, \beta) h(\alpha' - \alpha) d\alpha \right] d\beta$$

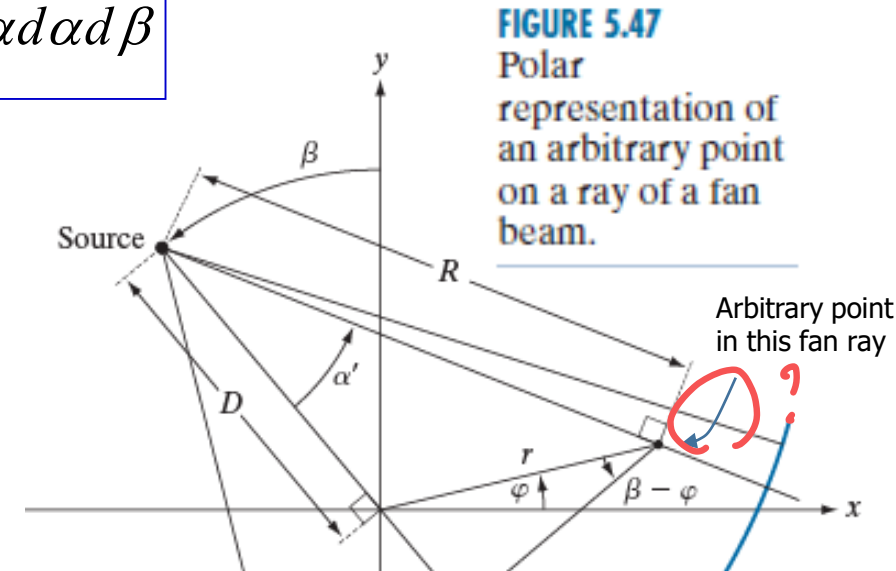


FIGURE 5.47
Polar representation of an arbitrary point on a ray of a fan beam.

$$\begin{aligned} r \cos(\alpha + \beta - \varphi) - D \sin \alpha \\ = r \cos(\beta - \varphi) \cos \alpha - [r \sin(\beta - \varphi) + D] \sin \alpha \\ = R \sin \alpha' \cos \alpha - R \cos \alpha' \sin \alpha \\ = R \sin(\alpha' - \alpha) \end{aligned}$$

Reconstruction Using Fan-Beam Filtered Backprojections (5)

Prove $s(R \sin \alpha) = \left[\frac{\alpha}{R \sin \alpha} \right]^2 s(\alpha)$, where $s(\rho)$ is the inverse FT of $|\omega|$.

Proof:

$s(\rho) = \int_{-\infty}^{\infty} |\omega| e^{j2\pi\omega\rho} d\omega$. Let $\rho = R \sin \alpha$. Note that $\frac{\alpha}{R \sin \alpha}$ is always positive. We have

$$\Rightarrow s(R \sin \alpha) = \int_{-\infty}^{\infty} |\omega| e^{j2\pi\omega R \sin \alpha} d\omega.$$

Let $\omega' = \frac{\omega R \sin \alpha}{\alpha}$. Then

$$d\omega = \frac{\alpha}{R \sin \alpha} d\omega'$$

$$\Rightarrow s(R \sin \alpha) = \left[\frac{\alpha}{R \sin \alpha} \right]^2 \int_{-\infty}^{\infty} |\omega'| e^{j2\pi\omega'\alpha} d\omega' = \left[\frac{\alpha}{R \sin \alpha} \right]^2 s(\alpha).$$

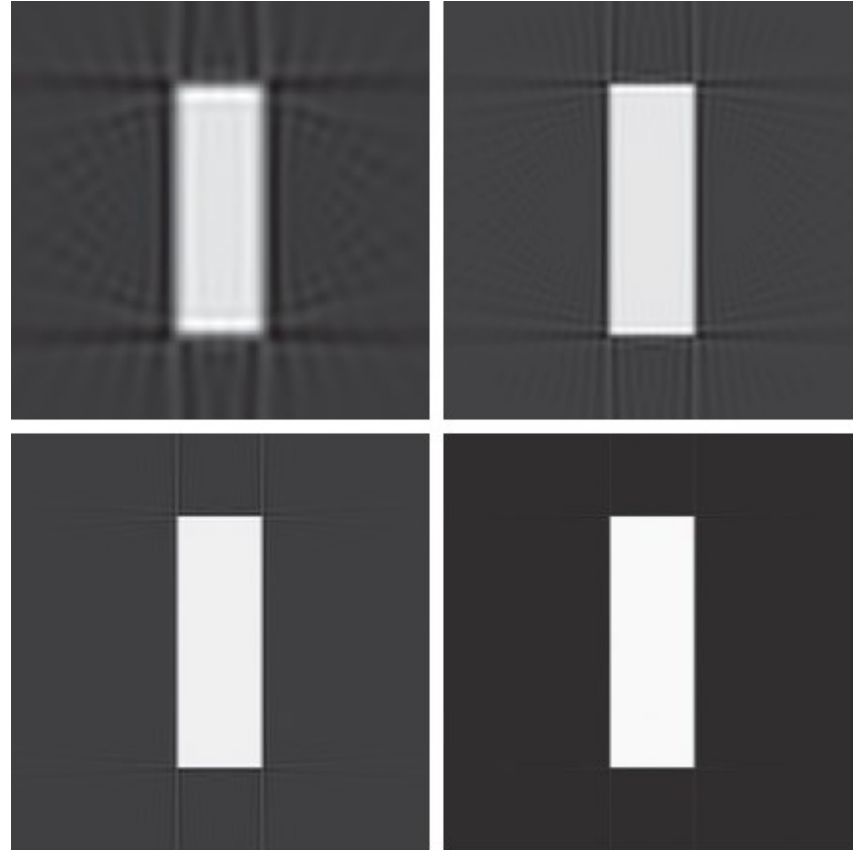
Reconstruction Using Fan-Beam Filtered Backprojections (6)

a
b
c
d

FIGURE 5.48

Reconstruction of the rectangle image from filtered fan backprojections.
(a) 1° increments of α and β .
(b) 0.5° increments.
(c) 0.25° increments.
(d) 0.125° increments.

Compare (d) with Fig. 5.43(b).



a
b
c
d

FIGURE 5.49

Reconstruction of the head phantom image from filtered fan backprojections.
(a) 1° increments of α and β .
(b) 0.5° increments.
(c) 0.25° increments.
(d) 0.125° increments.
Compare (d) with Fig. 5.44(b).

